TOPICAL REVIEW • OPEN ACCESS

Orbital angular momentum of twisted light: chirality and optical activity

To cite this article: Kayn A Forbes and David L Andrews 2021 *J. Phys. Photonics* **3** 022007

View the article online for updates and enhancements.

Journal of Physics: Photonics

TOPICAL REVIEW

Orbital angular momentum of twisted light: chirality and optical activity

Kayn A Forbes[1] and David L Andrews[1]

School of Chemistry, University of East Anglia, Norwich Research Park, Norwich NR4 7TJ, United Kingdom
[1] Correspondence may be addressed to either or both authors.

E-mail: k.forbes@uea.ac.uk and d.l.andrews@uea.ac.uk
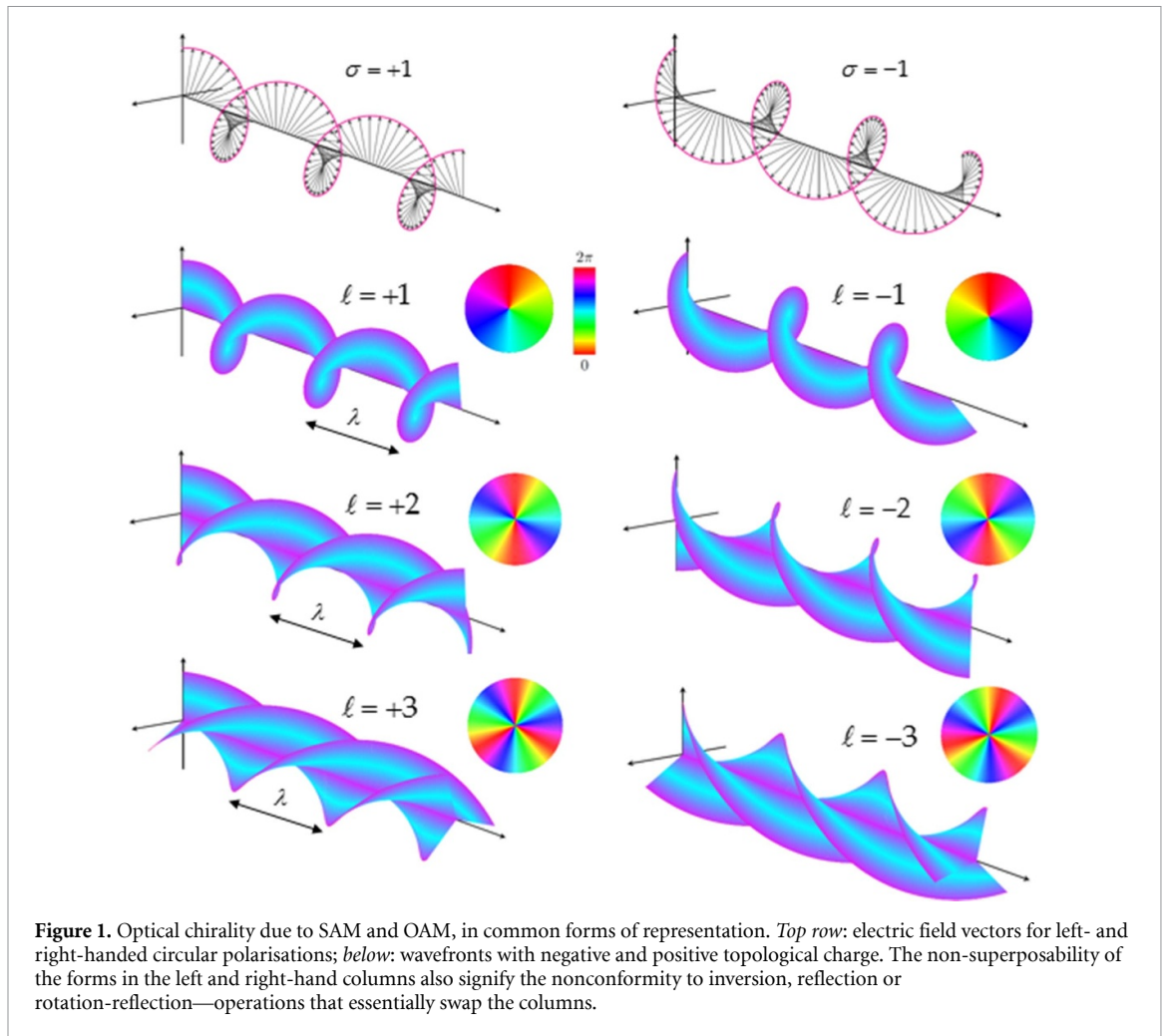
Abstract

Optical activity is conventionally understood as a natural difference in the optical responses of chiral materials with opposite handedness. It stems from the quantised spin angular momentum $\pm\hbar$ per photon, with the $\pm$ representing either left- or right-handed circular polarisations. Less well known, until recently, was the possibility that matter might also respond in a similar, discriminatory way to the handedness of twisted light, or 'optical vortices', whose *orbital* angular momentum (OAM) is quantised as $\ell\hbar$ per photon, where ℓ is the topological charge whose sign determines a wavefront twist to the left or right. Initial studies focusing on whether, in spectroscopic applications, chiral matter might respond differently to the vortex handedness of $+\ell$ and $-\ell$ beams, failed to identify any viable mechanism. However, in the last few years, theory and experiment have both supplied ample evidence that, under certain conditions, such forms of interaction do exist—and as a result, the field of chirality and optical OAM is beginning to flourish at a pace. This topical review presents a survey of this new field, working up from a description of those initial studies to the cutting-edge experiments now taking place. Analysing the fundamental mechanisms provides for a revision of previous precepts, broadening their scope in the light of recent advances in understanding, and highlighting a vibrant synergy between the fields of optical activity and twisted light.

1. Introduction

The dynamical characteristics of photons passing through any optical system, or individual component, necessarily conform to one of the supported modes of optical propagation. Whether in vacuum, crystal or fibre, or indeed any other optical element, each photon is simply a quantum excitation of one such mode. In addition to the universal modal attributes of quantised energy and linear momentum, the quantifiable properties of individual photons also include optical angular momentum—a property that, until the latter years of the twentieth century, was primarily conceived as a manifestation of photon spin. Due to the association of forward propagation with spin angular momentum (SAM), the optical helicity in the electromagnetic fields was widely understood as the basis for all chiroptical or gyrotropic forms of interaction with matter, i.e. processes sensitive to the relative handedness of circularly polarised light and chiral (mirror-asymmetric) matter. However, the discovery that photons might additionally convey integer amounts of orbital angular momentum (OAM), a development that quickly unlocked new areas of research in twisted and structured light, optical vortices, and singular optics [1], led to questions over potential connections between OAM itself, and chiroptical forms of light–matter interaction.

SAM is manifest through circular-polarisation states with a value of $\sigma\hbar$ per photon along the propagation axis: these are the only number states that diagonalise the optical spin operator [2]. The associated twist in the optical fields is denoted by $\sigma = \pm 1$, in which the sign registers a clockwise (right-handed) or anticlockwise (left-handed) rotation of both the electric and magnetic field vectors, as the light propagates towards the observer [3]. Under the symmetry operations of the three-dimensional rotation-reflection group O(3), such field structures lack invariance under inversion, reflection or rotation-reflection, fulfilling the

Figure 1. Optical chirality due to SAM and OAM, in common forms of representation. *Top row*: electric field vectors for left- and right-handed circular polarisations; *below*: wavefronts with negative and positive topological charge. The non-superposability of the forms in the left and right-hand columns also signify the nonconformity to inversion, reflection or rotation-reflection—operations that essentially swap the columns.

criteria for a 3D chiral structure. OAM, by contrast, generally originates from a wavefront folding into a helicoidal surface, with an integer topological charge (also termed 'winding number') $\ell \in \mathbb{Z}$ designating the number of such intertwined surfaces, each a wavelength apart—see figure 1. In an analogous fashion to the spin, the OAM per photon along the axis of propagation given by $\ell\hbar$ has a sign corresponding to the direction of twist: for $\ell > 0$ the vortex is left-handed; for a right-handed vortex $\ell < 0$. Here, the wavefront structure becomes invariant under C_ℓ longitudinal rotations, i.e. rotations (with an ℓ-fold symmetry) about the propagation axis: nonetheless, the lack of any other O(3) symmetry elements other than rotations again signifies a 3D chiral structure. Clearly then, rotations of either the electromagnetic field vectors or the wavefront in a helical fashion suggests a capacity for the exhibition of two distinct, and in principle distinguishable, types of optical chirality. Nonetheless, caution is required: careful analysis of the quantum operators reveals that although SAM and OAM are separately measurable, only their sum constitutes a genuine angular momentum [4–6], whilst only in the paraxial approximation is the simple decomposition of the total optical angular momentum into SAM of $\sigma\hbar$ and OAM of $\ell\hbar$ per photon legitimate (see section 6).

The differences in effect of optical spin and OAM are well illustrated by the observation that a trapped particle can be made to rotate around its centre of mass due to SAM, or around the centre of a beam owing to OAM [7], respectively, akin to the diurnal and annual rotations of the Earth in its planetary orbit. More intriguing differences arise in connection with the transfer of optical OAM to internal electronic degrees of freedom in simple systems [8], contrasting with the well-known connection between the unit spin of the photon and conventional electric dipole selection rules. Despite a multipolar character in the structure of many forms of complex light [9], the character of electronic transitions are governed by selection rules based on the symmetry of the material system. For example, it has been established that individual photons clearly need not convey OAM to produce, or be produced by, quadrupole electronic transitions [10]. The more intricate relationship that exists between multipole character and electronic selection rules is itself a topic of wide interest [8, 11–14]. However, such studies are mostly concerned with atomic systems, in which the electronic states have specific quantum attributes of angular momentum. The situation becomes much more

complex for twisted light interactions with molecules, where electronic states will often have symmetry representations spanning more than one specific value of OAM. Such complexity is compounded for molecules or materials of chiral form, and in consequence the interplay of chirality and optical OAM has become a subject of rapidly increasing traction.

The well-established mechanisms by which circularly polarised light interacts with chiral matter provide a variety of means for distinctive discrimination between enantiomers, i.e. forms of material with opposite handedness [15]. The less familiar role that the vortex handedness of optical OAM beams prove to offer in chiroptical and optical activity phenomena is the subject of this topical review. The sections that follow afford a survey of this new field of chirality and the OAM of light, including a historical perspective beginning with the very first studies and ranging up to the very recent and flourishing experimental and theoretical developments. In section 2, we first discuss the deeply entwined subjects of chirality and angular momentum in optics, specifically identifying mechanisms that are distinctly dependent on either SAM, OAM, or the total AM, and the nature of their relationship with multipolar interactions. Section 3 surveys the field of twisted light and natural optical activity, whilst section 4 deals with the role of OAM in magnetic optical activity. Section 5 highlights the important role that plasmonics has shown to exhibit in chiroptical effects sensitive to optical OAM. In contrast to the studies in sections 3–5 that directly depend on OAM, section 6 looks specifically at the role that the inseparable spin and orbital AM manifest in non-paraxial and spin–orbit coupled beams of light, in generating optical activity dependent on the sign of ℓ.

It will become apparent that we are witnessing a confluence of two strands of scientific development—structured light and the manifestations of chirality in light–matter interactions—that were, at least until the turn of this century, quite separate. As has become evident, posing the question of any possible synergy has led to several new discoveries, engendering what is now a vibrant field of research activity. Section 7 concludes with a discussion highlighting prospects for an exciting future, and some of the emerging avenues for further development.

2. Chirality, optical angular momentum and multipole interactions

The chirality of light, and its manifestations in light–matter interactions, has fascinated scientists for centuries. Following early nineteenth century reports on observations of chiral light–matter interactions by Arago [16] and Biot [17], it was quickly established that, individually, chiral molecules must be responsible for the distinctive polarisation effects produced by chiral crystals (optical rotation). It was Fresnel [18] who discerned a realistic mechanism involving a chiral aspect of light itself, associated with spin. Optical rotation, the chiral effect with which light is most familiarly associated, is itself observed with plane polarised light—but the underlying notion of a superposition of oppositely handed circular polarisations, propagating through material with different refractive indices for each handedness, is prevalent in standard textbook treatments [19]. More generally, it is now well understood that every physical effect attributable to optical chirality or optical activity and chiral discrimination owes its origin to the fundamental $\mathcal{CPT}$-symmetry invariance that holds sway across the whole field of optics [20–22]. Here, C signifies the operation of charge conjugation, $\mathcal{P}$ is spatial parity transformation, and $\mathcal{T}$ is time reversal.

Considerations of spatial parity, $\mathcal{P}$, provide a direct route to the comprehension of chiroptical interaction. Since several different kinds of optical activity and chiral discrimination emerge—not all of them necessitating an engagement with intrinsically chiral matter—it is appropriate to very briefly clarify the connection between fundamental symmetry and a common 'mirror image' understanding of optical activity in a molecular context. The internal geometry of a molecule is clearly invariant to rotation of the whole, and the operation of spatial inversion $\mathcal{P}$ combined with rotation by π radians is equivalent to mirror reflection; accordingly, the criterion of molecular inversion symmetry is more often considered as superposability upon a mirror image. The failure of this criterion by chiral species establishes the distinguishability of mirror-opposite *enantiomers*, conventionally designated right- and left-handed. The application of this principle obviates the awkwardness of discerning any specific 'chiral centre' within a molecule, supposedly responsible for lack of invariance under $\mathcal{P}$: more detail is provided in [22].

It is well known that every photon interaction is mediated by multipolar forms of engagement between the associated optical fields and the dynamic charge distributions of matter—the latter, in the UV-visible range, being determined by nanoscale electronic structures. The electric dipole approximation, so widely prevalent in conventional optics, of course represents but the most common leading contribution to a series of higher order terms. It is also possible to describe such multipole interactions by a 'minimal coupling' formalism, giving equivalent results, but the multipolar form much more directly links to observables, and it most readily elucidates chiroptical forms of interaction [23–26]. In brief, the coupling between light and matter described by the interaction Hamiltonian is representable in terms of the series;

Table 1. Space and time parity of electromagnetic quantities.

Operator	Time parity $\mathcal{T}$	Space parity $\mathcal{P}$
Hamiltonian H	$+1$	$+1$
Electric field $\boldsymbol{e}$	$+1$	-1
Electric multipole transition En	$+1$	$(-1)^n$
Magnetic field $\boldsymbol{b}$	-1	$+1$
Magnetic multipole transition Mn	-1	$(-1)^{n-1}$
Angular momentum $\boldsymbol{J}$, $\boldsymbol{L}$, $\mathbf{S}$	-1	$+1$

$$H_{\text{int}} = -\underbrace{\varepsilon_0^{-1}\boldsymbol{\mu}.\boldsymbol{d}^{\perp}}_{\text{E1}} - \underbrace{\varepsilon_0^{-1}\boldsymbol{Q}:\nabla\boldsymbol{d}^{\perp}}_{\text{E2}} - \underbrace{\varepsilon_0^{-1}\boldsymbol{O}\vdots\nabla\nabla\boldsymbol{d}^{\perp}}_{\text{E3}} - \ldots - \underbrace{\boldsymbol{m}.\boldsymbol{b}}_{\text{M1}} - \underbrace{\boldsymbol{m}^{(2)}:\nabla\boldsymbol{b}}_{\text{M2}} - \ldots, \tag{1}$$

where E1 represents the electric dipole transition moment operator $\boldsymbol{\mu}$ coupling to the transverse electric displacement field operator $\boldsymbol{d}^{\perp}$ (electric dipole interaction); E2 and E3 are the electric quadrupole and electric octupole couplings, respectively, both of which are dependent on the gradients of the electric field; M1 and M2 are the corresponding magnetic couplings between the magnetic multipole transition moment operators $\boldsymbol{m}^{(n)}$ and the magnetic field operator $\boldsymbol{b}$ and its gradient. The electric multipole moments in (1) come from the electric polarisation field of the material and the magnetic multipole moments from the magnetisation field; clearly both involve a linear dependence on the respective electromagnetic field operator indicating that each coupling involves a single photon. Equation (1) is exact, except in its exclusion of a diamagnetisation term involving the magnetic field interactions of two photons—which, since it is even in both space and time, cannot differentially engage in chiral interactions: its role in other optical connections is a newly emerging topic [27].

The electric and magnetic fields become operators in the quantum representation of light, now cast as Fourier expansions over a complete set of radiation modes. The operator mode expansion for the transverse electric displacement field for a paraxial Laguerre–Gaussian (LG) beam is [28]:

$$\boldsymbol{d}^{\perp}(\boldsymbol{r}) = i\sum_{k,\eta,\ell,p}\left(\frac{\hbar ck\varepsilon_0}{2A_{\ell,p}^2 V}\right)^{1/2}\left[\hat{\boldsymbol{e}}^{(\eta)}(k\hat{\boldsymbol{z}})\,a_{\ell,p}{}^{(\eta)}(k\hat{\boldsymbol{z}})f_{\ell,p}(r)\,\mathrm{e}^{(ikz+i\ell\phi)} - \text{H.c.}\right], \tag{2}$$

where H.c. denotes Hermitian conjugate; $\hat{\boldsymbol{e}}^{(\eta)}(k\hat{\boldsymbol{z}})$ is the electric polarisation unit vector; $a_{\ell,p}{}^{(\eta)}(k\hat{\boldsymbol{z}})$ is the annihilation operator (its Hermitian conjugate being the creation operator); $f_{\ell,p}(r)$ is a radial distribution function; p is the radial mode index integer whose value indicates the $p+1$ number of concentric rings of intensity in a LG beam; $A_{\ell,p}^2$ is a normalisation constant; V is the quantisation volume; and $\mathrm{e}^{(ikz+i\ell\phi)}$ is the optical phase, the azimuthal dependent part being responsible for optical OAM. In view of the emphasis that we shall place upon the interactions of vortex beams, it is worth emphasising that the transversality of the electric displacement field in (2), denoted by the symbol $\perp$ represents universal orthogonality specifically with respect to the local disposition of the Poynting vector—which in the case of twisted beams in general departs locally and systematically from the direction of beam propagation [29]. The need to make this distinction is a consequence of working in the Coulomb gauge as typical of non-relativistic light–matter interactions; magnetic fields are transverse regardless of gauge.

The interaction Hamiltonian (1) plays into a quantum amplitude for each optical process, casting the observable, such as a rate, or signal intensity, in terms of material transition moments and their products [22]. This is where clear and important differences arise in the symmetry properties exhibited by material multipoles of each form (not to be confused with multipole radiation). As an energy operator in QED, H_{int} has even parity both in time and space: accordingly, the $\mathcal{P}$ and $\mathcal{T}$ parity signatures of each multipole transition moment are the same as those of the electromagnetic fields and field gradients with which they engage. Electric multipole moments of odd order—dipole E1, octupole E3, etc—have components of opposite sign for chiral materials of exactly opposite handedness (enantiomers), whereas those of even order—quadrupole E2 etc—have the same sign for each chiral form. The opposite is true for magnetic transition moments; for example magnetic dipoles, M1, have the same sign for each species of enantiomer. The parity signatures of key properties are summarised in table 1.

For any optical interaction between *chiral* matter and circularly polarised light, if the quantum amplitude were to involve solely one form of transition moment (e.g. E1E1), the corresponding rate—quadratically dependent on its modulus—would be the same for both enantiomers. However, when more than one transition multipole features in a quantum amplitude, the lack of spatial inversion symmetry in interference terms such as E1M1 or E1E2 in the rate equation can give rise to differential effects, according to material

handedness. There is one readily explicable exception to this principle, of an unusual and especially interesting kind: the above rules relate to molecular components whose individual optical responses and transitions involve their material entirety, engaging the chirality or other symmetry of the whole system. However, in groupings or arrays of suitably disposed, chemically identical units, then even if the discrete units are achiral, the group may comprise a chiral whole. A circular array of n components may for example have C_n symmetry. Given electronic coupling between the units, the electronic energy levels in such a composite will split into an exciton structure with different quantities of electronic angular momenta in each level. Here, chirality of the system as a whole can be exhibited through purely electric dipolar coupling of each unit with radiation. Nonetheless, an equivalent formulation of the optical response in terms of the *entire system* would still engage E1M1 and E1E2 interference. Some interesting recent developments are based on such systems, and we shall return to discuss them in section 7. The higher symmetry of atoms and achiral molecules on the other hand means that they cannot engage in natural optical activity through the multipole transition moment interferences as chiral molecules do. However, they may still engage in other forms of optical activity, such as magnetic optical activity, where additional stimuli are present in the system: preservation of total parity dictates that at least two entities of odd parity in either $\mathcal{P}$ or $\mathcal{T}$ must always be present in the total light–matter system in order to yield differential phenomena.
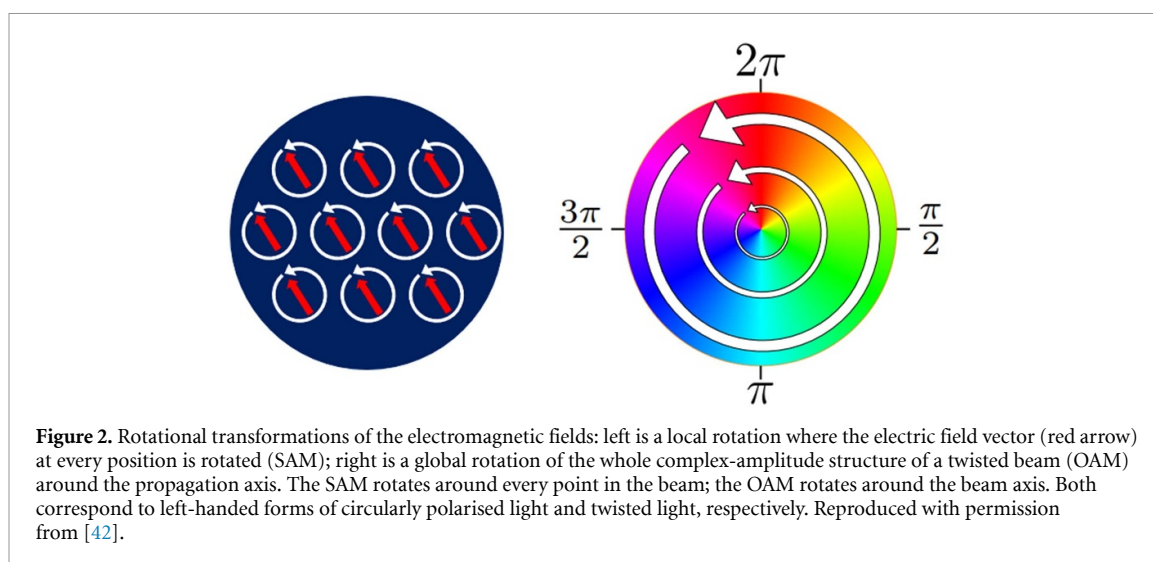
At this juncture it is also important to recognise that the term 'chiral', most widely and historically deployed to denote a lack of spatial inversion symmetry, is also now applied in a time-reversal sense of symmetry under operation $\mathcal{T}$—to signify direction-dependent propagation [30, 31]. In this connection there is some risk of miscomprehension in a burgeoning new usage of the terms 'left-handed' or 'chiral', which has already become prevalent in a wide range of recent optics literature, to signify a system in which the refractive index is negative. For the propagation of light through such, perhaps more informatively termed 'negative index metamaterials' [32–34], it appears that the linear momentum and energy flux are disposed in mutually opposite directions. The significance of the 'handedness' in this sense is argued from the vector product form of the defining the Poynting vector [35].

Fundamental photonics and electrodynamics clearly indicate that all the most familiar forms of optical chirality and optical activity are determined by the SAM of the light, linked to the helicity of the electromagnetic field [36]. By contrast, the chirality of optical vortices has been utilised in a plethora of material applications such as techniques for chiral fabrication [37], and the optical manipulation of matter: on the whole, these effects are inherently mechanical. In such applications, positive or negative OAM engages with motional degrees of freedom of the bulk material, in principle no differently from the effect of a screwdriver or wrench. In order to observe chiroptical and optical activity effects, however, we require angular momenta to be transferred to or from the internal degrees of freedom of the material. At the fundamental level, this generally signifies direct photon interactions with local, bound electrons. Alternatively put, we are looking specifically at how the OAM can affect the rates of optical processes, such as absorption, in contrast to very well-known mechanical effects in which the OAM does not increase or decrease the rate of spectroscopic processes, rather it induces and influences mechanical motion of the particles. An important aspect of this difference is that there are no constraints on the choice of detector; there is never any need to probe any OAM in the throughput or output.

The total angular momentum of any light field is a constant sum of both spin and orbital parts, and although the SAM and OAM are well-defined in monochromatic paraxial optics, they are not well-defined in general [6]. The spin is an intrinsic property of photons due to being bosons; OAM of light has both intrinsic and extrinsic components [38]. The SAM rotates the electromagnetic field vectors locally in space, and for freely propagating paraxial light it is directly related to a scalar property known as optical helicity, κ, defined as a volume integral of the inner product between vector potential and magnetic field [39]. In fact, in the paraxial approximation, it transpires that for any beam—irrespective of topological charge—the result for κ can be explicitly cast in terms of a difference between the number of left- and right-handed circularly polarised photons [36, 40]:

$$\kappa = \frac{\hbar}{\varepsilon_0 c} \sum_{\boldsymbol{k}} \left[N_{(\boldsymbol{k})}^{(\mathrm{L})} - N_{(\boldsymbol{k})}^{(\mathrm{R})} \right]. \tag{3}$$

In the absence of material interactions, this helicity is a conserved property. It is notable that, although it is a gauge of chirality, this parameter—like energy—is even under $\mathcal{P}$ and $\mathcal{T}$. However, its values map to the set of integers $\mathbb{Z}$, the sign designating handedness. Still more important is the fact that, unlike energy, linear momentum or angular momentum, there is no material counterpart, nor any quantum operator, for this property. Therefore, helicity is not in any quantifiable sense transferred to or from matter through any kind of optical interaction, whether or not they are sensitive to chirality. To further emphasise this point, it is notable that in the widely studied conventional case of Raman optical activity, the sign of the circular

Figure 2. Rotational transformations of the electromagnetic fields: left is a local rotation where the electric field vector (red arrow) at every position is rotated (SAM); right is a global rotation of the whole complex-amplitude structure of a twisted beam (OAM) around the propagation axis. The SAM rotates around every point in the beam; the OAM rotates around the beam axis. Both correspond to left-handed forms of circularly polarised light and twisted light, respectively. Reproduced with permission from [42].

intensity differential is usually found to change continuously, even over small intervals in the spectrum [41]. Although this differential is directly proportional to the optical helicity as defined by equation (3), the frequency-dependent fluctuations in sign of the scattering result from molecule-specific variations in the response functions.

By contrast the optical OAM generates rotations of spatial distributions of light, and is a global property. The difference in this sense, between the locality of SAM and the global quality of OAM is illustrated in figure 2. It is interesting to observe, however, that whilst there exists an optical helicity and chirality, and corresponding helicity and chirality density with respect to SAM, directly analogous aspects of OAM are seemingly not possible [36].
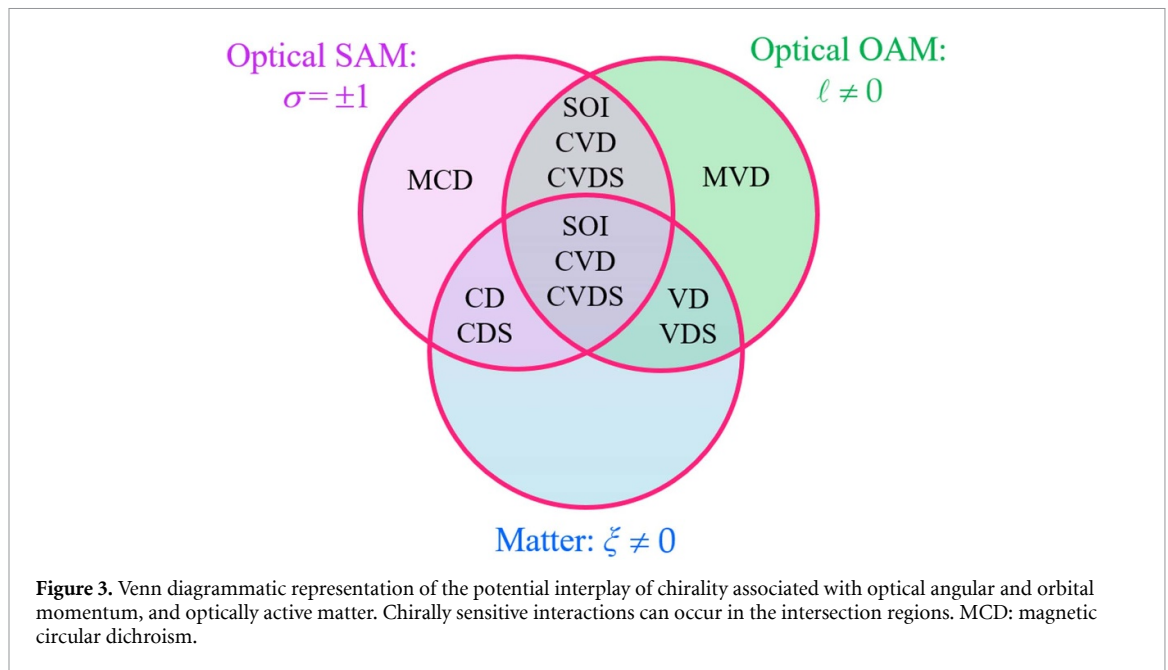
In general, accommodating the possibility of orbital as well as SAM contributions to chiroptical effects provides the basis for a fourfold categorisation of mechanisms. Such effects can either be dependent solely on SAM, or on OAM alone, or on both—the latter prospect providing grounds for a possible involvement of coupled spin–orbit interaction (SOI) signifying the exhibition of features not attributable to either form of angular momentum independently. Each category is distinguishable, since SAM and OAM are under entirely separable experimental control. The potential interplay of chirality associated with optical angular and orbital momentum, and optically active matter, is illustrated in the form of a Venn diagram in figure 3, in which the four distinct intersection regions correspond to the fourfold categorisation. Here we denote σ as a label for the helicity associated with SAM: material handedness (i.e. the quality of being non-superimposable on the form obtained by spatial parity inversion) is specified by non-zero ξ—implicitly ± 1 for left/right handedness according to arbitrary convention, and $\xi = 0$ for an achiral system.

Finally, before reviewing the field it is worth commenting on the varying terminology and acronyms found throughout the literature at present. In this review we label the OAM part responsible for any chiral effect as 'vortex', in preference to 'orbital' or 'helical', though all three terms are commonly used in the literature and generally mean the same thing. For single-photon absorption that is chirally sensitive to circular-polarisations alone we use the well-established phrase 'circular dichroism', ascribing it the usual acronym 'CD'. If that same effect additionally exhibits a dependence on optical OAM, we refer to it as circular-vortex dichroism 'CVD', rather than circular-helical or circular-orbital dichroism. An effect depending solely on OAM, we term vortex dichroism 'VD', rather than orbital or helical dichroism. Any effect due to magnetic optical activity is given the identifier 'magnetic', e.g. MVD is magnetic vortex dichroism. Also, we use the term 'dichroism' to strictly denote a resonant, absorption process, consistent with its original meaning: many recent authors use the term more loosely, to mean any differential response to CPL, whether absorption or scattering. We will make clear in the text which process is responsible. Any study based on measurements of transmission will generally conflate absorption and scattering effects.

3. Twisted light and natural optical activity

3.1. General principles of discriminating optical vorticity

The role of molecular chirality and stereochemistry has been deeply imbedded in the developing historical conception of optical activity phenomena. From origins early in the 19th century, right through to modern day applications, natural optical activity and chiroptical effects have been effectively used to probe the chiral

Figure 3. Venn diagrammatic representation of the potential interplay of chirality associated with optical angular and orbital momentum, and optically active matter. Chirally sensitive interactions can occur in the intersection regions. MCD: magnetic circular dichroism.

electronic structures of molecules—and, since the development of Raman optical activity and vibrational CD in the 1970's and 80's, the internal nuclear configurations of molecules, too [43–45]. Natural optical activity effects exhibited by chiral molecules (as opposed to magnetic optical activity associated with Faraday effects: see section 4) usually involve interferences between a dominant electric dipole (E1) form of coupling to the electromagnetic field, and two others: magnetic dipole (M1) and electric quadrupole (E2)—see equation (2). The latter of these interferences—E1E2—have *in general* been overlooked on account of the fact that, given random molecular orientations (such as in a liquid), they commonly average to zero, unlike the E1M1 contributions which persist [23, 44].

It was with a focus on E1M1 that Andrews and co-workers reported the first analysis on twisted light and optical activity [46] in 2004, restricting initial considerations to the dipole approximation. Their theory looked at the simplest of processes, single-photon absorption, considering whether light possessing OAM might exhibit an analogue of the CD that arises when chiral molecules are subjected to circularly polarised light. The crux of this initial issue was this: do such molecules absorb photons with $+\ell$ at a different rate than those with $-\ell$? The study, looking specifically at paraxially propagating LG structured light, for which a molecular quantum electrodynamical formalism had previously been developed [28], discovered that within the dipole approximation, neither chiral nor achiral molecular matter could engage the vortex handedness (i.e. the sign of ℓ) of a twisted light beam.

This theoretical prediction was substantiated with an experimental study the following year, which measured the CD of an isotropic solution containing a chiral bisquinone derivative of helicene, using both non-OAM possessing Hermite–Gaussian (HG) modes and LG modes [47]. It was determined that for HG and LG light, both circularly polarised, there were no differences in the observed CD. The results proved to be in full agreement with the theory of Andrews *et al*—verifying that the OAM does not engage in the CD of isotropic chiral molecular matter. Interestingly this was not the first experimental attempt at observing optical activity due to optical OAM. Padgett and Allen had done work in 1993 that went unpublished, in which they failed to observe optical activity from a solution of sugar molecules subjected to an unpolarised twisted light beam [48].

Recently, the electrodynamic mechanism was reappraised for single-photon absorption involving OAM photons, going beyond the dipole approximation to include contributions from electric quadrupole transitions [49]. The electric quadrupole (E2) interaction is the first and most significant term in the multipolar expansion that depends on the transverse gradients of the electric field in the interaction Hamiltonian (within the paraxial regime). E1 and M1 coupling can be approximated as $\boldsymbol{\mu} \cdot \boldsymbol{d}^{\perp} \approx \boldsymbol{\mu} \cdot \hat{\boldsymbol{e}} f_{\ell,p}(r) \, \mathrm{e}^{(ikz+i\ell\phi)}$ and $\boldsymbol{m} \cdot \boldsymbol{b} \approx \boldsymbol{m} \cdot \hat{\boldsymbol{b}} f_{\ell,p}(r) \, \mathrm{e}^{(ikz+i\ell\phi)}$. However, the form for E2 coupling is more complicated due to the gradient operator, and we exhibit its form here as an illustration of the tensorial structures that arise in such interactions:

$$\boldsymbol{Q} : \nabla \boldsymbol{d}^{\perp} \equiv Q_{ij} \nabla_j d_i^{\perp} \approx Q_{ij} \nabla_j \hat{e}_i f_{\ell,p}(r) \, \mathrm{e}^{(ikz+i\ell\phi)} = Q_{ij} \hat{e}_i \left[\hat{r}_j \partial_r + i\ell r^{-1} \hat{\phi}_j + ik\hat{z}_j \right] f_{\ell,p}(r) \, \mathrm{e}^{(ikz+i\ell\phi)}. \tag{4}$$

In the terms on the right of the first equality, expressions are cast in the Einstein convention of implied summation over repeated (subscript) directional indices i and j. From the form of this equation it is evident that the electric quadrupole transitions may be driven by both transverse (r, ϕ) and longitudinal (z) phase gradients, and importantly the former consist of helical-phase gradients with a linear dependence on the topological charge ℓ of the beam. This indicates that the rate of single-photon absorption (and other light–matter interactions) can in fact be dependent on the OAM content of an input paraxial vortex, both its magnitude and sign. It is pivotal to recognise that this term, dependent on the topological charge, engages the azimuthal component of the canonical momentum density [38, 50], and thus engagement of E2 interactions (to the most significant order) allow the locally-extrinsic nature of the OAM to be probed in non-mechanical light–matter interactions. The radial gradient has no connection with phase, and so in its engagement with the electric quadrupole it cannot directly engage chirality, and furthermore for any well-collimated paraxial beam its absolute contribution is negligible.

In the ensuing calculations, the interference terms that arise in the modulus square of the Fermi rate rule for photon absorption, i.e. $\Gamma \propto |\text{E1} + \text{M1} + \text{E2}|^2$, permit a CD analogue for twisted light, termed CVD. This feature is distinctively dependent on the product $\sigma \cdot \ell$ that arises in the E1E2 contributions to photon absorption. In other words, this contribution to the rate of absorption for a chiral molecule is opposite in sign for twisted photons of $+\ell$ and $-\ell$, and the difference also scales linearly with $|\ell| \hat{\phi}_j / r$. It is also important to note that the effect only exists for circularly polarised twisted light: with plane polarised light a spin-independent VD is possible, but only through higher order multipolar contributions, namely pure quadrupole, E2E2. Clearly the E1E2 interferences are the lowest-order multipolar contributions to optical processes with which OAM can engage, and therefore represent the most easily experimentally observed. Higher-order contributions, dependent on the vortex handedness for both chiral and achiral molecules, have recently been derived for absorption and scattering [51, 52]: their identification represents an additional experimental challenge.

In an analogous fashion to CD and optical rotation with light possessing no OAM, the E1E2 contribution to photon absorption vanishes upon a three-dimensional molecular orientational average [53] and, as it is the sole contributor to CVD, this effect vanishes too in isotropic systems. It is therefore evident why the early theory and experiments failed to observe any influence of optical OAM on CD and optical rotation in chiral molecular liquids, as not all of the necessary criteria were fulfilled. The engagement of E2 interactions is requisite; the molecular system needs to display some degree of orientational order (e.g. not an isotropic fluid)—and the input twisted light has to be circularly (or at least elliptically) polarised. The distinction in behaviour between isotropic fluids (liquids and solutions) and orientationally ordered, or partially ordered systems such as the domains in liquid crystals, often proves pivotal in the criteria for observing chiroptical effects dependent on sign of the OAM. It hinges on the ergodic theorem, which in this respect establishes connection between a local ensemble average and the time-average response of individual constituent molecules.

Shorter-wavelength light allows higher-order multipole contributions, beyond the electric dipole, to become important due to the spatial variations of the electromagnetic field becoming more influential over molecular dimensions. With this in mind Ye *et al* [54] used a minimal coupling analysis to computationally study, via *ab initio* calculations, CVD as a probe of molecular chirality (the molecule cysteine in this case), with x-ray pulses of twisted light. They also studied pure VD. Comparing CD, VD, and their CVD results, they found that in general CVD gives stronger signals compared to CD, and that the main contribution to the signals stem from molecules positioned close to the phase singularity. Their analysis includes all multipolar contributions, yielding results predicting that these effects will actually persist in isotropic chiral molecular systems through higher-order multipoles. This conclusion is consistent with the QED theory cast in multipolar form [51]—however, the very small size of these higher-order interactions indicates another reason why experiments have often failed to observe these effects in isotropic solutions of chiral molecules.

With the quadrupole paradigm discovered, further studies have investigated the role that optical OAM might play in the *scattering* of twisted light by chiral molecules [42, 55]. The prominent optical activity phenomena due to the molecular scattering of circularly polarised light are Rayleigh and Raman optical activity [44], otherwise known as circular differential scattering (CDS). These processes involve the differential rate of scattering of left- versus right-handed circularly polarised photons that originates from interferences between the E1E1 couplings involved in the molecular polarisability α with the mixed E1M1 and E1E2 molecular polarisabilities, G and A, respectively [23, 44]. For incident paraxial light with optical OAM, it was discovered that a differential scattering effect dependent on the product $\sigma \cdot \ell$ exists through the αA contribution to scattering: circular-vortex differential scattering (CVDS). Importantly, in contrast to CVD, CD, and optical rotation in which only the E1M1 contribution persist in isotropic molecular systems,
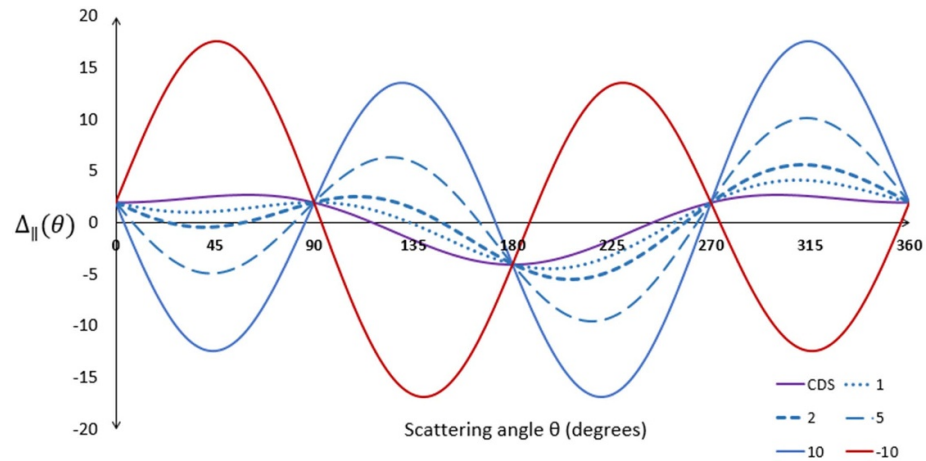
Figure 4. Plot of CVDS differential scattered intensity $\Delta I = I^{\ell}_{\sigma(L)} - I^{\ell}_{\sigma(R)}$ of light with $\hat{k}\hat{k}'$-plane polarisation components against scattering angle (indicative case of $(kr)^{-1}\cos\phi = 1$). Varying the topological charge values (1, 2, 5, 10) highlights the difference in scattered intensity enhancement for high values of ℓ, and also shows how this changes with scattering angle. The shift in maximum scattering differences stems from a simple increase in the weighted contribution of the CVDS effect as ℓ increases. The chiroptical scattering effect with respect to the vortex handedness is displayed through the plots for $\ell = \pm 10$. These effects are relative for the fixed radial position, normalised against the dominant electric-dipole scattering mechanism (i.e. Rayleigh or Raman scattering).
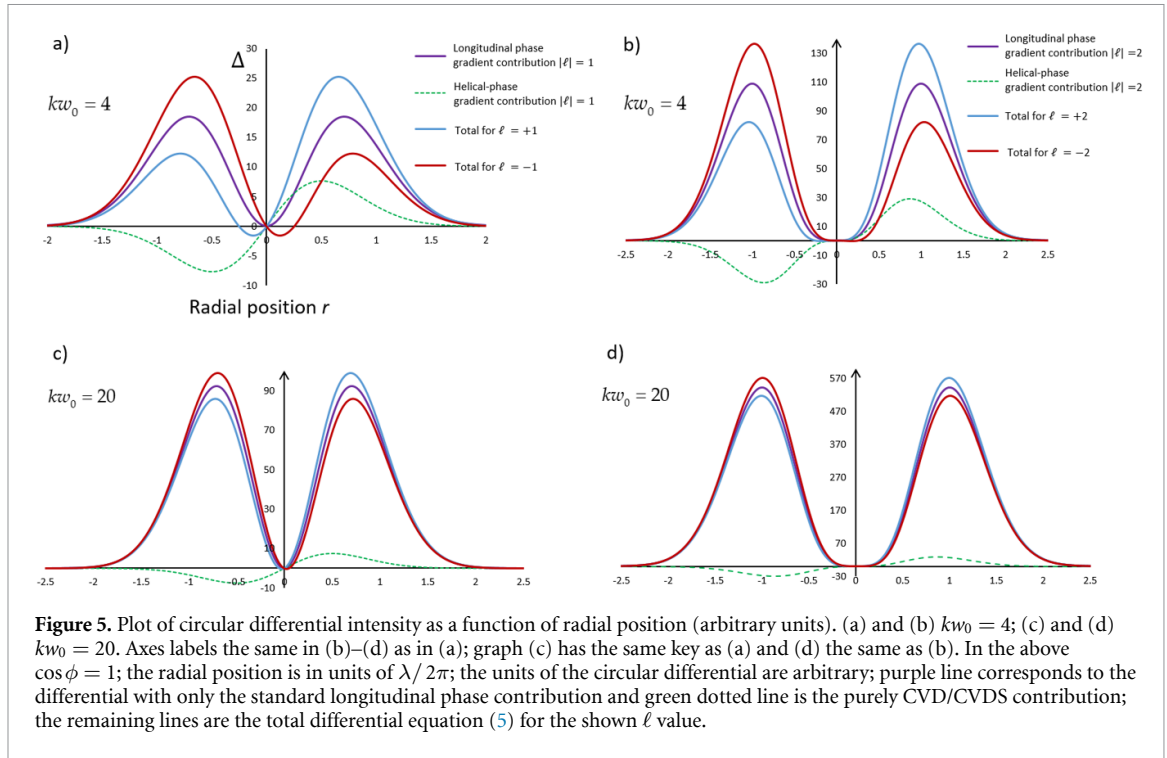
for CVDS and CDS both E1M1 and E1E2 (αA) contribute to the scattering, for both anisotropic and isotropic systems.

One way to observe CDS and CVDS in the laboratory is through a measurable difference in the scattered intensity of input LCP and RCP light $\Delta I = I_{\sigma(L)} - I_{\sigma(R)}$. (For unfortunate reasons in the history of CDS, the differential is commonly defined in the opposite sense, right minus left: for internal consistency in this survey, we adopt the former definition.) In this experimentally measurable quantity CVDS has numerous features that differ from CDS. Firstly, the intensity of scattering produced through CVDS has a different scattering-angle dependence (see figure 4); the CVDS effect depends on both the sign and magnitude of the OAM, and thus offers an enhancement of signals for high-OAM input, and the capacity for measurement of the scattered intensity difference between ℓ and $-\ell$; CVDS, unlike CDS, cannot be observed for scattered light that is polarised transverse to the scattering plane; and finally, CVDS, in contrast to CDS, has a further dependence on molecular position within the transverse beam profile, through the factor $\ell r^{-1}\cos\phi$ for orientationally averaged systems, and it is therefore highly sensitive to the both the radial and azimuthal location.

The $\sigma \cdot \ell$-dependence of both CVDS and CVD means that it is possible to define a scattered intensity vortex difference $\Delta I = I^{\ell(L)}_{\sigma(L/R)} - I^{\ell(R)}_{\sigma(L/R)}$ where the input circular polarisation state is fixed, but the topological charge $|\ell|$ is modulated between positive and negative values—such vortex modulation is now experimentally viable [56]. This method of studying the optical activity of twisted light should more readily allow its distinctive features to be quantified experimentally, as it separates off the standard optical activity effects that depend solely on the sign of circular polarisation.

There is one other possible approach to the detection of chiral response due to a vortex-structured beam. Just as in standard circular-differential optical activity studies, where circular polarisation components of the scattered light may be studied (*scattered circular polarisation optical activity*) [57], there is potential scope to measure the different scattered intensities for various OAM states of the output light. Although in general the OAM of the scattered light is not conserved, the theory does predict small differences in scattered vortex modes [52]. Though this will more than likely be very technically demanding, it should offer even further insights into the structure of the material scatterer. Similarly, it has been highlighted through numerical simulations that it is possible to distinguish, in a system of locally ordered particles partially eclipsing the beam focus, between domains with chiral or non-chiral arrangements. This is achieved by controlling the input OAM, and measuring the power of specific OAM modes of the output scattered fields in the far-field zone [58]. However, possible sensitivity to the chirality of the individual particles remains an open question.

Not long after CVD and CVDS were discovered, Alfano's group carried out extensive studies on the transmission of LG beams through different regions of mouse brain tissue [59]. The transmission rates exhibit a clear dependence on ℓ, characteristics of which are indicative of a CVD- or CVDS-type interaction. Exploratory experiments studying Raman optical activity in anisotropic chiral solids with vortex beams have

Figure 5. Plot of circular differential intensity as a function of radial position (arbitrary units). (a) and (b) $kw_0 = 4$; (c) and (d) $kw_0 = 20$. Axes labels the same in (b)–(d) as in (a); graph (c) has the same key as (a) and (d) the same as (b). In the above $\cos \phi = 1$; the radial position is in units of $\lambda / 2\pi$; the units of the circular differential are arbitrary; purple line corresponds to the differential with only the standard longitudinal phase contribution and green dotted line is the purely CVD/CVDS contribution; the remaining lines are the total differential equation (5) for the shown ℓ value.

also exhibited some results that tally with the anticipated properties of CVDS [60, 61]. The most recent theoretical study in this area highlighted that CVDS can occur in *nonlinear* scattering by chiral molecules: hyper-Rayleigh and hyper-Raman optical activity of optical vortices [62]. This study constitutes the first study on nonlinear optical activity with twisted light.

3.2. Radial position dependence

There are important common features of both CVD and CVDS optical activity effects with regards to the radial position of the molecules within the laser beam profile that invite further consideration, as they deliver deeper physical insights into the practicality of observation. As we have discovered, for any light–matter interaction, the pursuit of a dependence on the handedness of a helical wavefront necessitates the engagement of an E2 coupling for a paraxial input twisted beam. To leading order, chirally sensitive effects can be produced from E1 couplings and a *single* E2 interaction, and this leads to a common motif in a circular-differential rate:

$$\Delta_{\text{L-R}} \propto N I^n(r) k \left(1 + \frac{\ell}{kr} \cos \phi\right), \tag{5}$$

where $I^n(r)$ is the input beam intensity (n is linked to the degree of optical nonlinearity: $n = 1$ for linear absorption and scattering, while $n = 2$ for second harmonic scattering or two-photon absorption, for example) and N is the number of molecules. The first term in the brackets of (5) is the contribution from the longitudinal phase gradient, common to both structured and unstructured light. The second term in (5) is unique to beams with a helical phase, where ℓ / kr is known as the skew angle [63] (see equation (4)). Whilst (5) is very general and highlights the key physics of the optical activity, it contains only the optical parameters of the system, and any specific result will contain the material responses which further influence the relative contributions of the two terms in (5) to the total differential.

Let us first consider the strong dependence on r, the radial displacement of the interacting particle from the beam axis. Firstly it is instructive to consider the range of positions necessary in order for the helical-phase term to contribute on a similar magnitude to the standard, non-OAM longitudinal phase gradient term. It is clear that since $k = 2\pi / \lambda$, the condition on equality imposes the criterion $r \approx \lambda / 2\pi$. For light in the visible range, this means chiral molecules positioned close to the vortex singularity contribute to the vortex-dependent mechanisms relatively much more than those positioned further away; The optimal positioning will be determined by the interplay of the ℓr^{-1} feature and the $|\ell|$-dependent radial distribution associated with the specific vortex mode (ℓ, p), including the beam waist w_0. Some indicative plots are exhibited in figure 5.
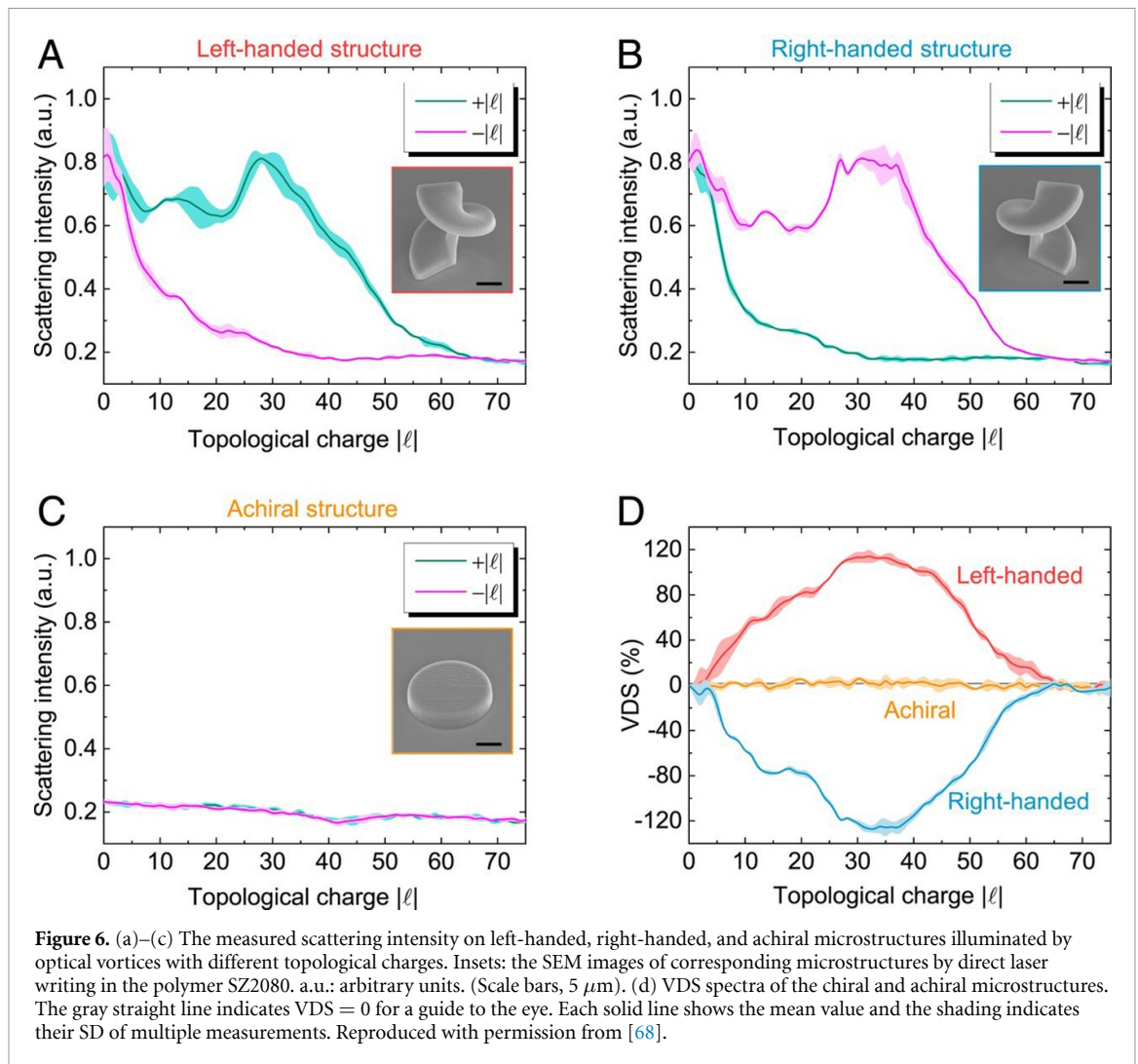
Figure 6. (a)–(c) The measured scattering intensity on left-handed, right-handed, and achiral microstructures illuminated by optical vortices with different topological charges. Insets: the SEM images of corresponding microstructures by direct laser writing in the polymer SZ2080. a.u.: arbitrary units. (Scale bars, 5 μm). (d) VDS spectra of the chiral and achiral microstructures. The gray straight line indicates VDS = 0 for a guide to the eye. Each solid line shows the mean value and the shading indicates their SD of multiple measurements. Reproduced with permission from [68].

For a given wavelength, as the beam waist w_0 is reduced, the relative magnitudes of the CVD/CVDS effects decrease with respect to the purely longitudinal phase gradient terms; however in the specific case of $kw_0 = 4$ for a wide range of values the CVD and CVDS effects clearly influences the overall differential in basically all radial positions. When the beam waist is increased to $kw_0 = 20$, any influence is only found at specific locations close to the highest intensity regions of the beam. The symmetry of the graphs clearly indicate that the total intensity difference for an OAM beam when integrated over the whole transverse profile is the same as if no CVD/CVDS mechanism was present.

Further ways to increase the effects include using smaller wavelength light, which will allow focusing that generates a smaller beam waist, on the scale of λ. Strong focusing, $kw_0 \leqslant 4$, will accentuate non-paraxial features, but although new physics can emerge through the modification of longitudinal components, the optical interactions stemming from the transverse structure, identified above, are not substantially affected [51]. Alternatively, it has been shown that optical vortices with large beam waists can be generated with a Gaussian intensity envelope embracing a point singularity at the centre [64], leading to vortex core size to beam waist ratios of $w_{VC}/w_0 \approx 0.02$. Another avenue is the use of plasmonic enhancements of metallic nanoparticles to enhance the coupling between chiral molecules and optical vortex light—we return to this in section 5. Moreover, systems that include plasmonic nanoantennas are currently being fabricated with the aim of breaking the diffraction limit for OAM light, and thus the generated nanovortices will be on a scale that matches molecular dimensions [65–67]. Alternatively, matching the dimensions of the material to that of optical vortices in the visible range has been shown to yield large rates of vortex differential scattering (VDS) [68]. Specifically, a single chiral microstructure with a size comparable to the beam waist exhibited a maximum VDS dissymmetry factor of $\sim 120\%$ when the input vortex mode had a topological charge $|\ell| \sim 32$ (figure 6).

3.3. Angular position dependence

Turning now to look at the angular dependence in equation (5), the $\cos\phi$ factor proves to be another extremely important feature of these interactions, again intricately linked to the fact the OAM of twisted beams is a spatial property, rather than a local one (section 2). It is readily evident that the transverse beam profile average of the vortex-related differential (integrating $\cos\phi$ over ϕ in the range 0 to 2π) is zero, reflecting an azimuthally oscillatory pattern with maximum values in the range $\pi/2$–$3\pi/2$. An interesting feature of the behaviour exemplified in figures 4 and 5 is that the sign of the whole plot changes if the observer rotates position by a 180 degrees around the beam axis, due to the $\cos\phi$ dependence. This serves as a reminder that in scattering experiments the azimuthal angle is no longer arbitrary; it is fixed by reference to the scattering plane. Therefore to strengthen the observed signal, an off-axis aperture may be required to partially eclipse the full beam, despite introducing some diffraction losses. Detection requires that either the totality of the beam profile should not be incident on the material sample, or that localised, offset regions of the illuminated sample output signal need to be probed. In other words, off-axis beam alignment, or a detection of signals stemming from only portions of the total beam [69] fulfils the condition for these effects to be observed. Furthermore, the integer number m of E2 couplings included in a light–matter interaction produces contributions to any optical process that are proportional to $\left(\ell r^{-1}\right)^{m}\cos^{m}\phi$ where $m = 1, 2, \ldots n$. For example, in the all of the optical activity effects discussed above, where we have been concerned with the leading order, most experimentally viable effects, the inclusion of only a single E2 coupling produces terms proportional to $\left(\ell r^{-1}\right)\cos\phi$. The next-highest order contributions produce a term dependent on $\left(\ell r^{-1}\right)^{2}\cos^{2}\phi$, and in this case the result clearly does not vanish over the transverse beam profile. However, since this effect depends on ℓ^{2} it is independent of the sign of the topological charge. By extension we can see that, if signals are collected uniformly across the input beam profile, the very small degree of engagement with the input beam vortex is only dependent on the modulus of $|\ell|$, not its sign.

4. Twisted light and magnetic optical activity

Isotropic systems of atoms and achiral molecules, subject to a spatially uniform static magnetic field, have a capacity to display magnetic optical activity. At a fundamental symmetry level the effects stem from the fields acting as an external time-odd influence (parity -1 under time reversal $\mathcal{T}$). The most famous example in optics is Faraday rotation; in the realm of spectroscopy it is best known through the differential absorption of circularly polarised light by both chiral and achiral matter: magnetic CD [70]. An early study in the field of twisted light and optical activity predicted an OAM-induced x-ray MVD in achiral matter [71]. The predicted MVD effect stems from purely quadrupolar transitions, which are strongly driven in materials subjected to twisted x-rays. This MVD enables the separation of quadrupolar and dipolar transitions, as was proven by numerical simulations for cuprates, manganites, and ruthenates, thus establishing its potential as an incisive probe of $3d$ states of transition-metal complexes. More generally, the strong OAM-induced dichroism highlights a novel non-dipolar spectroscopic technique to study orbital physics and magnetism.

In an experiment published in 2013, Mathevet and co-workers [72] attempted to observe such an MVD effect in Nd^{3+} ions in a YAG host. The transition they studied is essentially electric dipole in nature, although, in atoms of this size, electronic SOIs undermine precise specification. Given the more recent QED studies discussed earlier [49], it is now clear to see why such an experiment returned negative results. Interestingly, in their article the authors postulated that electric quadrupole moments, at the lowest order, should give rise to a MVD—and as we have seen, the theory of van Veenednaal and McNulty is in full agreement [71]. It is highly noteworthy to observe that even in magnetic optical activity effects with twisted light, the electric quadrupole and interactions with the gradient of the fields are necessary to observe chiroptical engagement of the vortex handedness.

A recent experimental study using terahertz optical vortices has highlighted how twisted light can couple to magnetised dysprosium iron garnet, which exhibits dichroism that is dependent on both the topological charge of the vortex and the magnetisation produced by Nd magnets. It is especially interesting that this directional MVD is stronger than that for circularly polarised light [73].

Finally, MVD stemming from a magneto-optical Kerr effect, which is the change in incident light reflected by a magnetised surface, has been theoretically studied for LG beams reflected off a non-homogeneous magnetised surface [74]. Three different types of dichroism exist in the reflected intensity pattern for the setup, which enables the chirality of magnetic structures to be determined without polarimetric analysis: MVD for a fixed magnetisation, but different sign of ℓ; a fixed sign of ℓ but opposite magnetisation; and the case where both are different. The effects originate from the spatially inhomogeneous magnetic structure redistributing the input single mode optical vortex into a spread of OAM modes (ℓ, p) in the reflected light. Again, the spatial nature of optical OAM is manifest, as integration over the scattered field leads to a null MVD result independent of the sign of OAM (or magnetisation). Therefore any MVD in this
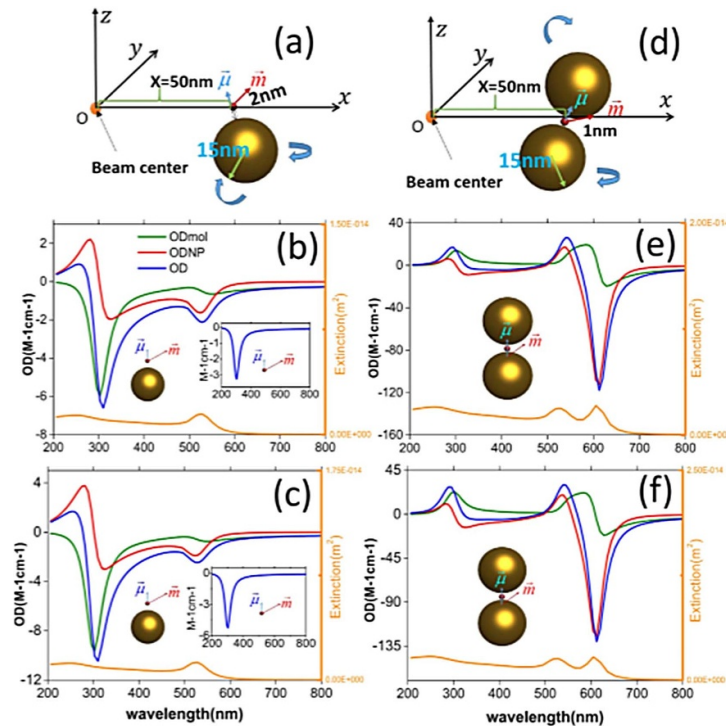
Figure 7. (a) System of coordinates and schematics of a complex composed of a gold nanoparticle and chiral molecule. (b), (c) Orientation averaged VD and extinction coefficients as a function of wavelength for a metal nanoparticle and chiral molecule under the OAM incident beam with $\ell = \pm 1$ and $\ell = \pm 2$, respectively. Insets represent the calculated results for the single chiral molecule without nanoparticles. (d) System of coordinates and schematics of a nanoparticle dimer and a chiral molecule. (e), (f) Calculated VD and extinction coefficients as a function of wavelength for the Au dimer and a chiral molecule in an OAM incident beam with $\ell = \pm 1$ and $\ell = \pm 2$, respectively. Nanoparticle radius 15 nm, pair separation 1 nm. Reproduced from [78]. CC BY 4.0.
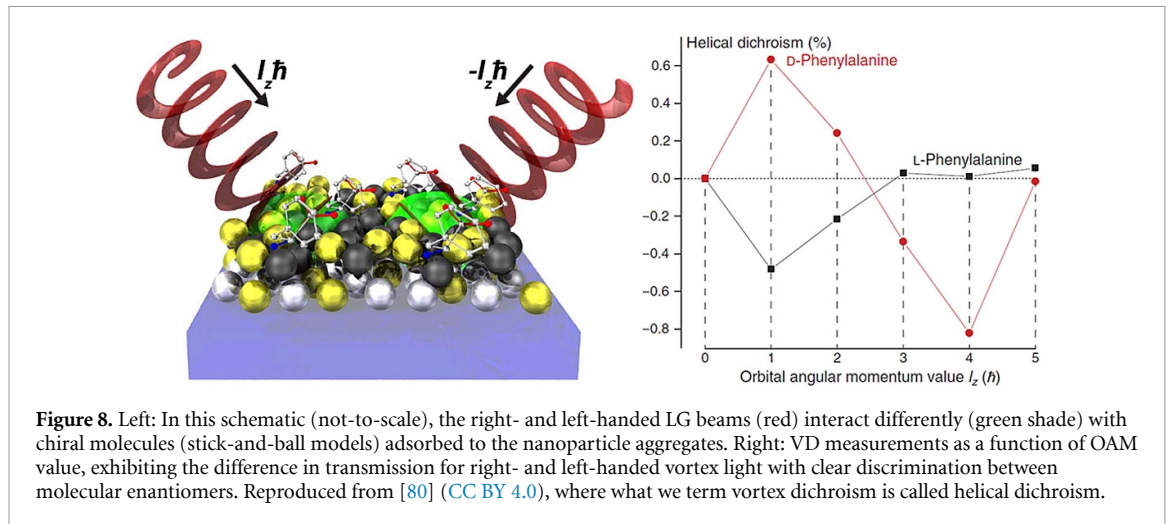
set up has to be determined from local single points in the far field. One particularly interesting example in these studies is the use of materials with an azimuthally-dependent magnetisation, so-called 'magnetic vortices' (not to be confused with optical vortices).

5. Plasmonics

As discussed in section 3, chirality and optical activity are intimately connected to geometrical molecular symmetry and structure: it is the nature of chemical bonds and the overlapping of atomic orbitals alone that lead molecules to possess a handedness. In comparison to natural structures, plasmonic metamaterials can offer significantly enhanced light–matter interactions, in addition to specifically chiroptical and optical activity effects [75–77].

The first study to look directly at the influence of surface plasmon resonances revealed a strong interaction induced between chiral molecules and twisted light. Using the T-matrix method, Wu *et al* [78] carried out in-depth numerical calculations modelling the absorption of focussed linearly polarised twisted light in a nanocomposite comprised of chiral molecules and metallic nanoparticles—see figure 7. A strong VD was discovered for randomly oriented molecules with a fixed position within the beam, due to the excitation of plasmon resonances in nearby nanoparticles, with enhancements of VD by a factor of 30 for chiral molecules in the hotspot of a plasmonic dimer (compared to the vicinity of a single nanoparticle). The sign and magnitude of the VD was seen to be highly dependent on geometrical configurations of the molecule-nanoparticle system, i.e. on the radial position of the nanocomposite in the cross-section of the OAM beam, where nanocomposites closer to the beam centre result in larger VD signals.

It is interesting that this study focused solely on dipole coupling by the molecules. Even with the aid of plasmonic nanoparticles, the VD completely vanishes upon a full transverse beam-profile average, as an equal amount of positive and negative signals are combined—as observed for molecules in the studies reported in section 3 and those for atoms in section 6—and in a further analogous manner the VD persists for nanocomposites of fixed orientations in defined regions of the beam. A more recent numerical study looking at CVDS in plasmonic cuboid-protuberance chiral structures also attributed the differential effects to dipole interactions, namely via the mixed electric magnetic dipole polarisability tensor $\boldsymbol{G}$ [79].

Figure 8. Left: In this schematic (not-to-scale), the right- and left-handed LG beams (red) interact differently (green shade) with chiral molecules (stick-and-ball models) adsorbed to the nanoparticle aggregates. Right: VD measurements as a function of OAM value, exhibiting the difference in transmission for right- and left-handed vortex light with clear discrimination between molecular enantiomers. Reproduced from [80] (CC BY 4.0), where what we term vortex dichroism is called helical dichroism.

In the pursuit of VD, Brullot *et al* [80] synthesised a layered composite of silver, gold and iron oxide nanoparticles, forming a plasmonic aggregate with a strong local electric quadrupole field due to near-field plasmon coupling between adjacent nanoparticles. First, these fields were shown to strongly interact with the magnitude of the optical OAM of the incident linearly polarised LG light. Then by adsorbing chiral molecules in the nanoparticle aggregates (see figure 8) the authors exhibited how the OAM can engage with molecular chirality only through electric quadrupole fields (and not a magnetic dipole field), enabling enantiomers to be resolved through VD, at wavelengths far from their CD resonances. The study specifically showed VD for the phenylalanine enantiomeric pair, exhibiting VD differentials of up to 0.6%, whereas standard CD values are generally in the range of 0.01%–0.1%.

Since chiral molecules exist naturally in enantiomeric pairs they give mirror-symmetric (positive and negative) optical activity spectra. However, synthetic chiral metamaterials are usually constructed with a single handedness, and so typically only exhibit either positive or negative signals. Ren and Gu [81] utilised the OAM of vortex light to produce giant 'bisignate circular dichroism' in a *nonresonant* AM mode-sorting nano-ring slit enclosed by a plasmonic nano-groove coupler. Their system works on the interplay between the topological charge of the OAM mode of the input light ℓ_{input} and the geometrical charge ℓ_{geo} of the plasmonic coupler. The CD signal in their experiment is defined as the transmission of LCP minus RCP for OAM-carrying beams through the nano-ring slit, and importantly: $\iota CD\iota^{L\text{-}R}_{\ell_{input},\ell_{geo}} = -\iota CD\iota^{L\text{-}R}_{-\ell_{input},-\ell_{geo}}$. The most striking case of this AM-dependent reversibility in differential transmission is when the geometrical topological charge of the nano-grooves is $\ell_{geo} = 0$ and the OAM of the input light is switched from $+2$ and -2: the results are shown in figure 9. It is clearly evident that the giant (up to 0.95%) response is completely reversed upon changing the OAM-handedness of the incident twisted beam. Furthermore, due to the dependence of the transmission on the geometrical topological charge of the nano-grooves, the study also proved that AM-reversibility exists by using $\ell_{geo} = \pm 1$ and $\ell_{input} = \pm 1$.

Numerical simulations on a very similar system to the study by Ren and Gu [81] highlighted AM-dependent transmission of circularly polarised vortex beams through a coaxial nano-ring [82]. These studies underscore the scope for engaging the handedness of vortex beams via coupling to the AM-conserving surface plasmon polariton modes.

Computational simulations of the strong coupling of circularly polarised LG beams, to a chiral plasmonic metasurfaces composed of subwavelength gold nanohelices, found that the total AM of the incident light and the vortex handedness had a strong influence on the dichroic response [83]. With a 543 nm input wavelength, the OAM-assisted CD shows a 200-fold enhancement compared to regular CD of a single nanohelix. The sign of the CD signal for $\ell = +1$ is the opposite for $\ell = -1$, whilst being approximately equal in absolute magnitude, showing that this is a CVD effect. For an array of helices, the CVD has a complicated dependence on the spatial separation of the structures, but for example with an input wavelength of 509 nm and 12 helices separated by 30 nm, the exhibited dichroism is almost an order of magnitude larger than for the same system with separations of 50 nm. The authors hypothesise that these effects stem from the OAM being transferred to the electronic degrees of freedom (the oscillations of the surface electrons) through a substantially enhanced quadrupole interaction with the plasmon resonance of the nanohelix.

Recently Arikawa *et al* [84] designed a metamaterial that allowed experimental proof that optical vortices can selectively excite multipolar modes in localised surface plasmons. By efficient OAM transfer, it was observed that $\ell = 1$ could selectively excite quadrupole modes and $\ell = -2$ hexapole, whereas unstructured
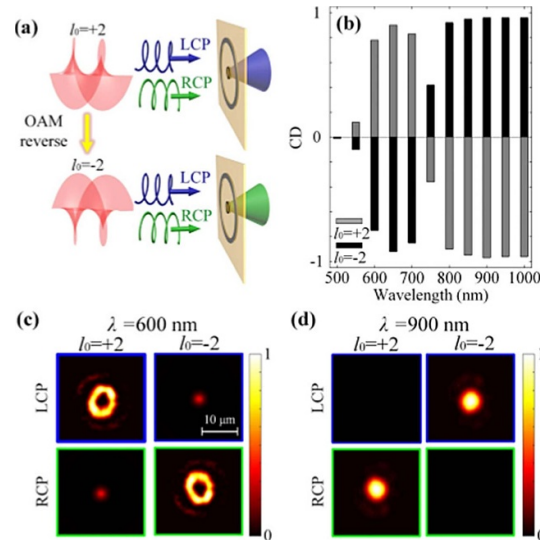
Figure 9. Experimental verification of AM-reversible transmission through changing the sign of the OAM in the case of a concentric plasmonic nano-groove coupler. (a) Schematic of a reversible transmission response achieved from using OAM modes with opposite signs ($\ell_{\text{input}} = \pm 2$) in incident light. (b) Experimentally measured transmission results for OAM modes $\ell_{\text{input}} = +2$ (grey) and -2 (black) at various wavelengths. Measured transmissive intensity patterns of OAM-carrying LCP and RCP beams at wavelengths of (c) 600 nm and (d) 900 nm, respectively. [81] John Wiley & Sons. © 2018 WILEY-VCH Verlag GmbH & Co. KGaA, Weinheim.
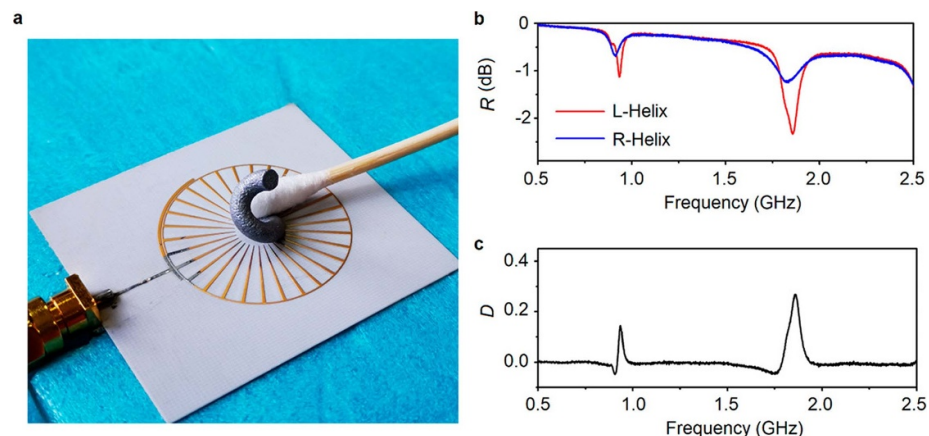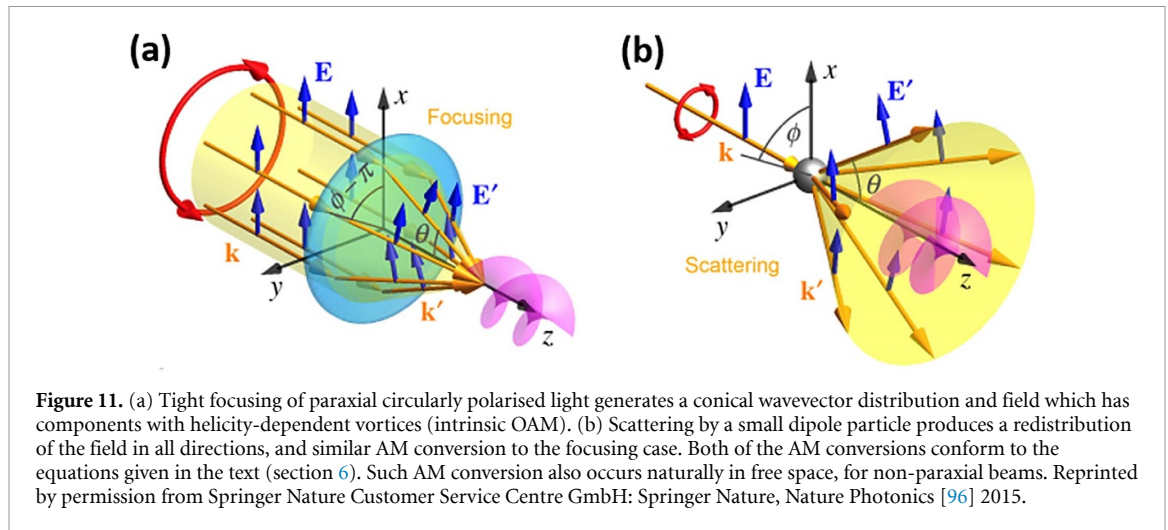

Figure 10. Dichroism experiment for the aluminium helices with a diameter of $\lambda/60$. (a) Photograph of the experiment. (b), (c) Experimentally measured reflectance (R) spectra and dissymmetry factor (D) where $D = 2(R_R - R_L)/(R_R + R_L)$. Reprinted with permission from [85]. Copyright 2020 American Chemical Society.

Gaussian light $\ell = 0$ could only excite dipole modes. The excited quadrupole modes were shown to correspond to localised surface plasmons that exhibited $2\hbar$ of angular momentum, one unit being transferred from each of the SAM and OAM of the incident beam. This work therefore provides evidence yet again that for optical OAM transfer to a material's internal electronic motion, quadrupole excitations (or higher multipolarity) are requisite [8, 11], and it consolidates the emerging explanations described in the earlier section dealing with plasmonics.

Finally Zhang and Cui [85] have observed a VD-type differential response for single chiral particles with diameters 60 times smaller than the wavelength using a microwave plasmonic resonater—see figure 10. Rather than studying direct OAM light–matter interactions like absorption and scattering, the highly-sensitive resonance OAM modes confined in the resonater are influenced by the presence of the chiral particle. Chiral meta-particles which possess the same handedness as the OAM mode lead to less disturbance and damping in the reflectance spectrum compared to when the OAM mode and material particle had opposite handedness. The work was specifically concerned with chiral meta-particles and microwave frequencies of light, however the authors believe their system can act as a blueprint for chiral biomolecules at optical frequencies.

Figure 11. (a) Tight focusing of paraxial circularly polarised light generates a conical wavevector distribution and field which has components with helicity-dependent vortices (intrinsic OAM). (b) Scattering by a small dipole particle produces a redistribution of the field in all directions, and similar AM conversion to the focusing case. Both of the AM conversions conform to the equations given in the text (section 6). Such AM conversion also occurs naturally in free space, for non-paraxial beams. Reprinted by permission from Springer Nature Customer Service Centre GmbH: Springer Nature, Nature Photonics [96] 2015.

6. Non-paraxial beams and SOIs of light

For a paraxially propagating beam the electromagnetic fields are approximated as being always perpendicular to the direction of propagation, and the intrinsic spin and orbital parts of the angular momentum are well defined [86–88]. However, for non-paraxial fields the local values of spin and OAM are not so readily separable [6], and the electromagnetic field distributions contain longitudinal components as a first-order correction to the zeroth-order transverse paraxial fields [89, 90]. For example, equation (2) in section 2 possesses $\hat{z}$ polarised components in addition to the transverse electric field displacement as a first post-paraxial correction. These field components are highly dependent on the beam structure [91] and are known to be pivotal in rigorously accounting for spectroscopic phenomena with non-paraxial sources [92, 93]. For an OAM-possessing Bessel or LG beam, for example, it is a degree of non-paraxiality associated with longitudinal fields that leads to an ℓ-dependent spatial distribution of helicity density [94]. This optical helicity in the focal plane can in turn result in the exhibition of optical activity in chiral structures. The SOIs in non-paraxial fields also generate a *spin-to-orbital angular momentum* conversion for circularly polarised beams, with a non-integer repartitioning of the spin and orbital components whose expectation values are representable as [95, 96]: $\langle S_z \rangle = \sigma \hbar \cos \theta$ and $\langle L_z \rangle = [\ell + \sigma (1 - \cos \theta)] \hbar$, where the outgoing wave-vectors of the light form a cone at an angle θ (figure 11).

In the limit $\theta = 0$, the result gives the well-known paraxial result that the spin and orbital AM are well defined and separable, whereas for $\theta = \pi/2$ there is a complete angular momentum conversion to OAM. In either case the total angular momentum $J_z = (\ell + \sigma) \hbar$, reflects the fact that the sum is a conserved quantity, in the free beam. The key physical manifestation of SOI that concerns us here is that part of OAM becomes helicity-dependent (i.e. dependent on the SAM), allowing for vortex light generation for incident beams even with $\ell = 0$.

Therefore, in non-paraxial beams of light there are a number of potential avenues to engage the chirality of twisted light through the topological charge ℓ: via electric quadrupole or higher multipolar moments of the material structure engaging with the gradient of the zeroth-order (paraxial) transverse field, specifically the helical phase gradient (as discussed in the previous sections); or through SOI and longitudinal fields.

The first experiments using highly-focussed non-paraxial vortex beams in the pursuit of optical activity were those undertaken by a group from the Netherlands. In their first study [97], Löffler, *et al* failed to observe any influence of optical OAM on CD of cholesteric polymers using either highly-focussed (non-paraxial) or well collimated (paraxial) circularly polarised LG beams. In their experiments they attempted to quantity any OAM influence on CD through an identification of $\delta_{\mathrm{OAM}} \propto \mathrm{CD}^{\mathrm{L-R}}_{\ell=+1} - \mathrm{CD}^{\mathrm{L-R}}_{\ell=-1}$. No influence of the sign of ℓ was observed in either the non-paraxial or paraxial experiment. One reason for the null result of their paraxial beam experiment can now be understood from the further advances in the theory highlighted in section 3: since the whole material sample was subjected to the beam, the corresponding circular-vortex component of the absorption rate averages to zero.

The second study by this group attempted to observe optical rotation of HG modes in a stratified multilayer chiral medium [98]. The motivation behind the experiment was the clever recognition that, just as the standard optical rotation of linearly-polarised light in chiral media can be understood by viewing the input as a superposition of left and right circular polarisations, the non-OAM possessing HG modes are also expressible as a superposition of opposite handedness LG OAM modes, ℓ and $-\ell$. In the experiment the
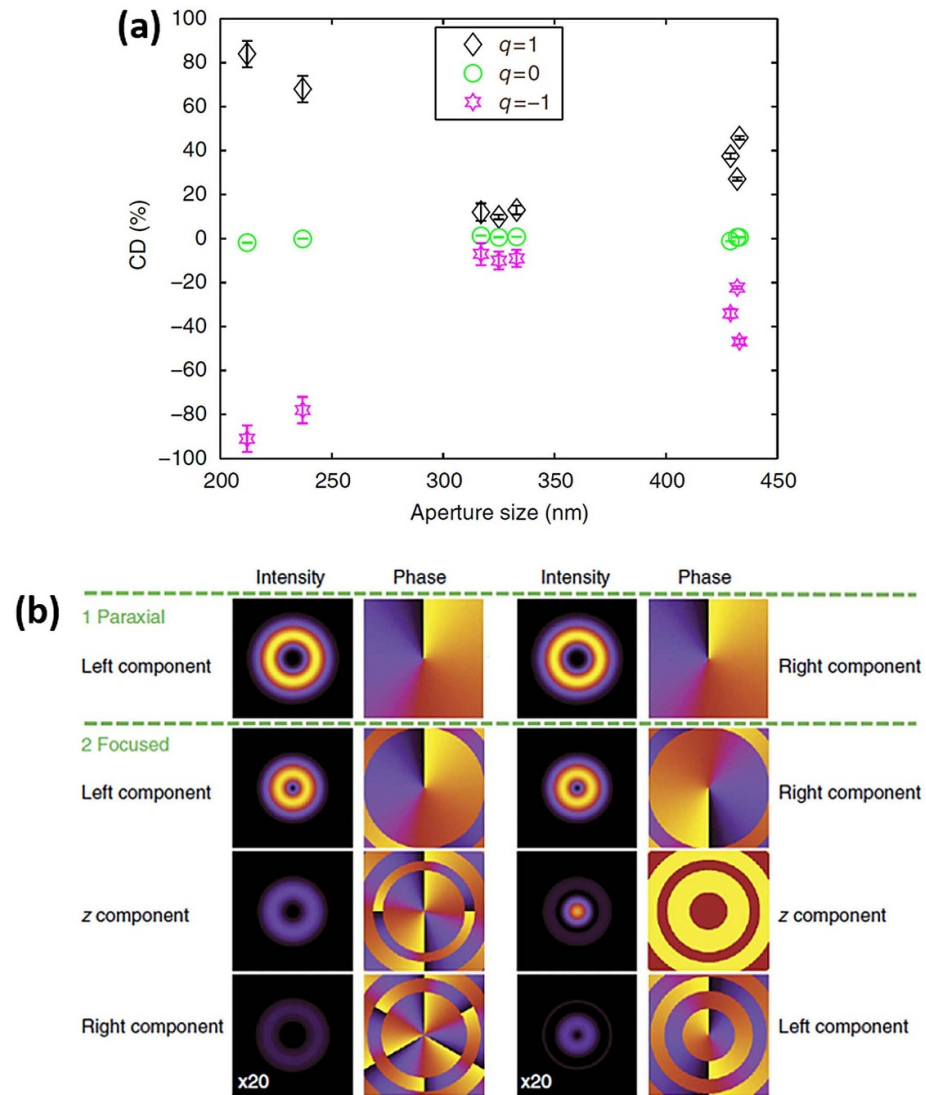
Figure 12. (a) Measurements of CD for three different values of optical OAM $\ell = q$ as a function of the diameter of the nano-aperture. Error bars are computed as the standard deviation of a set of 20 measurements with the same sample. (b) Intensity and phase plots of the two beams: left-hand columns $\sigma = 1, \ell = 1$, right-hand columns $\sigma = -1, \ell = 1$. Upper row shows the paraxial intensity and phase distributions for the two beams. In contrast, the bottom three rows show the intensity and phase distributions for the same beams, at the focal plane. Although their paraxial intensities and phases are analogous, the structures are completely different and non-mirror-symmetric at the focal plane—a direct consequence of SOI. Reprinted by permission from Springer Nature Customer Service Centre GmbH: Springer Nature, Nature Communications [99] 2014.

relative phase delay of OAM light with different handedness is measured after passing an incident HG beam through a cholesteric liquid crystal, (with a pitch, i.e. a full 2π rotation on the order of the optical wavelength), and studying the rotation of the nodal line of the HG beam. Again, both in the paraxial and non-paraxial regime, the helically-arranged liquid crystal polymers failed to mediate HG mode rotation via optical rotation. It is interesting to speculate as to why no optical rotation of HG modes is observed in this chiral cholesteric system. Although no specific microscopic theory of optical rotation with twisted light has yet been developed, it is well known that for chiral matter with orientational order, E1M1 and E1E2 interactions are responsible to optical rotation and as such, akin to CVD and CVDS, one might equally expect the sign of OAM to be able to engage in the system studied by Löffler *et al* through the quadrupole contribution. However, the null result is again potentially explicable by the issues discussed in the previous paragraph, particularly the effective averaging of ϕ.

In an experiment by Zambrana-Puyalto *et al* [99] a microscope objective lens (N.A. = 1.1) was used to focus a beam with both SAM and OAM ($\ell = \pm 1$) leading to a helicity-dependent intensity distribution through SOI [100]. This beam was then incident upon non-chiral plasmon nanostructures comprising subwavelength circular apertures of varying diameters. Giant induced 'circular-dichroism-like' signals were observed (see figure 12(a)) that stem from the fact that the input beams $\ell = \sigma$ and $\ell = -\sigma$ are not mirror images of each other in this non-paraxial regime (as exhibited in figure 12(b)), and in theory

$'\mathrm{CD}'^{\mathrm{L\text{-}R}}_{\ell} = -'\mathrm{CD}'^{\mathrm{L\text{-}R}}_{-\ell}$ (Here, the inverted commas signify that measurements are based on transmission, essentially conflating the dichroic effects of absorption and scattering). For $\ell = 0$ there was found to be no $'\mathrm{CD}'^{\mathrm{L\text{-}R}}_{0}$ of the achiral structures, as would be expected from parity considerations alone. An interesting feature of the experiments was that the CD (transmission) is positive when $\ell = \sigma$ whilst negative for $\ell = -\sigma$. This is a rather non-intuitive observation in that the transmission of a vortex mode with $|J_z| = 2$ and an intensity null in the centre is greater through the nanoholes than a $J_z = 0$ mode with maximum intensity at its centre; however similar behaviour has been previously observed [101]. The full interpretation of such experiments is only possible by taking into account the highly distinctive features that arise in any form of optics involving sub-wavelength apertures [102]. The non-monotonic dependence on the aperture radius may well stem from the dissimilar focused fields coupling differently to the multipolar moments of the material, a phenomenon well-known in Mie theory. Potentially of a similar origin involving the superposition of multiple multipolar modes, it has been observed that the spectral features of Mie scattering from TiO$_2$ spheres is independent of the sign of ℓ for low OAM values, but dependent on the sign for high values, such as $\ell = \pm 6$ and ± 7 [103].

Another experiment utilising the OAM of light to indirectly probe material chirality engages so-called *spin-orbit beams* developed by Samlan *et al* [104]. Using a polarisation Sagnac interferometer, vector vortex beams (beams with inhomogeneous polarisation) were generated with non-separable SAM and OAM and an azimuthal phase gradient. Measuring the rotation of beam intensity of an off-centred LG vortex against a reference enabled them to determine the optical rotation of quartz, as it has a one-to-one correspondence with the vortex mode rotation: significantly, the rotation direction (clockwise or anticlockwise) is dependent on the vortex handedness.

In studies that engage spin–orbit coupling with plasmonic interactions, Kerber *et al* [105] numerically studied what they defined as four different classes of 'dichroism' with a highly-focussed Bessel beam in varying geometries of monomer, dimer, and trimer stacked pairs of plasmonic nanoantennas—see figure 13, in which the spin state is labelled s rather than σ. Although the term 'dichroism' is strictly associated with resonant absorption processes, the 'dichroism' they study is in fact differential scattering with circularly polarised vortex beams. The four classes of CVDS studied involve: CDS of circularly polarised light with a fixed value of ℓ; differential scattering with fixed circular-polarisation for the input light and absolute value of $|\ell|$ but variable sign; a 'parallel class' of differential scattering where $\ell = \sigma$; and an 'anti-parallel class' where $\ell = -\sigma$. The simulations highlight the fact that in the case of the monomer aligned with the beam axis, only the standard, OAM-independent CDS mechanism exists. For dimers and trimers, however, OAM-dependent differential scattering is found. For dimers there is a small VDS that is one order of magnitude weaker than normal CDS: for the trimers, whose results are illustrated in figure 13, the CVDS with a fixed circular polarisation is now of the same order as CDS, and thus the nanostructure can differentiate the sign of ℓ. There also exists a differential scattering for the parallel and antiparallel combinations of spin and angular momentum, the uniqueness of which stem from SOI and helicity-dependent intensity distributions. All of the effects display an angular dependence on the angular displacement between the nanoantennas within each pair, such that the nanostructure becomes achiral at $\alpha = 0, 90°$.

Afanasev *et al* [106] studied the theory of CD produced by twisted photons in strictly non-chiral atomic matter. With the atomic targets subjected to non-paraxial circularly polarised Bessel beams, it was discovered that a CD dependent on the OAM (i.e. a form of CVD for achiral matter) only occurs for interactions involving purely electric quadrupoles or higher multipoles. These calculations indicate that this atomic CVD increases for increasing values of input ℓ, and also in general when θ becomes larger, though it still remains large in the *paraxial* limit and is in fact effectively independent of θ for values below ≈ 0.25 rad. Furthermore, this study indicated that the CVD is largest for atoms positioned near the centre of the beam, peaking at the phase singularity. As we would expect, if the atomic position were not resolvable, full integration over the beam profile will lead to a null result for atomic CVD. Mechanisms that exhibit very similar properties have also been highlighted in achiral molecular matter, stemming from purely E2 absorption and higher-order scattering effects with paraxial light [51, 52]. Here also there are strong echoes of the principles of E1E2 chiral molecular CVD, enunciated in section 3.

Rather than using a spin-to-orbit AM conversion, in their elegant study Wozniak *et al* [107] used the OAM to local non-zero optical chirality conversion that occurs in a tightly focussed linearly polarised LG beam, to excite a chiral nanostructure solely through electric and magnetic *dipole* interactions. The SOI utilised in their experiments engages longitudinal field components and a non-zero optical helicity along the optical axis, whose sign is dependent on whether the incident beam is $\ell = 1$ or $\ell = -1$. Thus a chiral nanostructure placed in the focal field can interact indirectly with the incident OAM. In the plot of their numerical simulations and experimental results shown in figure 14, there is a clear difference between the transmittance of $\ell = 1$ and $\ell = -1$ for a sub-wavelength chiral gold nanohelix. This differential interaction
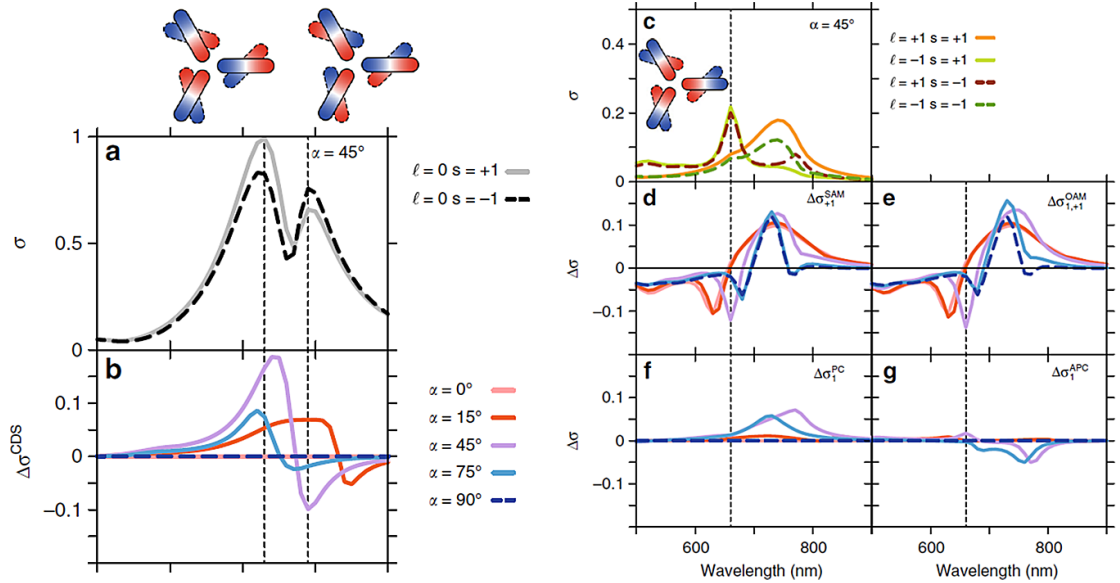
Figure 13. (a) Scattering cross-section spectrum for a nanoantenna pair displacement angle $\alpha = 45°$ for beams with $\ell = 0$ and $s = \pm 1$: (b) and circular differential scattering $\Delta\sigma^{\mathrm{CDS}}$ for a trimer of nanoantennas. (c) Scattering cross-section spectrum for an angle $\alpha = 45°$ for Bessel beams with $\ell = \pm 1$ and $s = \pm 1$. (d) Spectra of four differential scattering effects as indicated: standard CDS $\Delta\sigma^{\mathrm{SAM}}$ for $\ell = 0$. (e) CVDS for a fixed value of SAM $\Delta\sigma^{\mathrm{OAM}}_{1,+1}$ for $s = +1$ and $|\ell| = 1$. (f) Differential scattering for the SOI cases of the parallel SAM and OAM $\Delta\sigma^{\mathrm{PC}}_1$ (f) and (g) the corresponding anti-parallel class $\Delta\sigma^{\mathrm{APC}}_1$. Reproduced from [105]. CC BY 4.0.
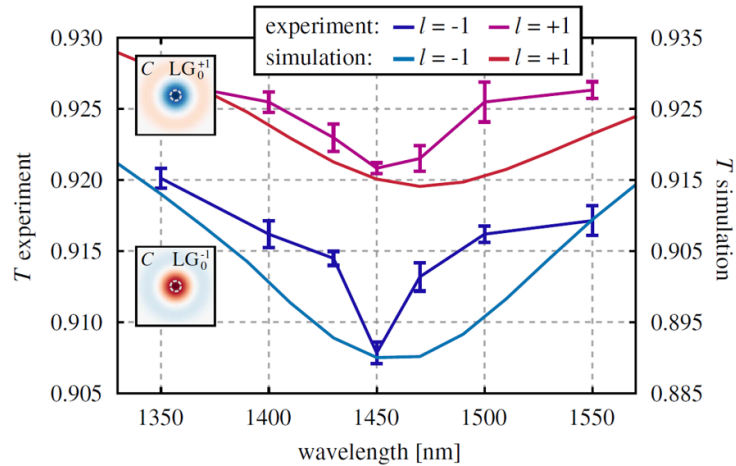

Figure 14. Experimental and simulation transmittance (T) spectra of the fundamental resonance of the right-handed nanohelix as a function of the vorticity of the incoming beam. The insets depict the focal optical chirality and the relative size and position of the nanohelix in the focal plane. Reproduced from [107]. CC BY 4.0.

arises because the mixed electric-magnetic dipole tensor **G** (a hallmark of optical activity—see section 3.1) exhibited by a chiral helix is dependent upon the material handedness, and can only be excited by either $\ell = 1$ or $\ell = -1$. The results in figure 14 relate to a right-handed helix, which strongly couples to input beams with $\ell = -1$; repeating the same experiment with a left-handed helix instead showed stronger coupling to an $\ell = +1$ input, as is to be expected on symmetry grounds.

Notably, theory work first highlighted this chiroptical capacity of longitudinal electromagnetic fields in non-paraxial optical vortices [108]. In their study, Rosales-Guzman *et al* showed how the longitudinal fields at the centre of a superposition of $+\ell$ and $-\ell$ linearly-polarised Bessel beams leads to an optical chirality that can interact with a chiral object to produce optical activity signals that are significantly enhanced, compared to standard chiroptical effects with circularly polarised light.

7. Conclusion and outlook

The most important conclusion to draw from this review is the unequivocal proof—from both theory and experiment—that the handedness of an optical vortex can interact in a chiroptical fashion with matter. Focusing on the most readily measurable processes of absorption and scattering, we have defined two clearly distinct kinds of mechanisms by means of which materials can exhibit optical activity with respect to the direction the vortex twists: mechanisms for paraxial electromagnetic fields which strictly require light–matter interactions that depend on transverse gradients of the field, the lowest-order of which is electric quadrupole couplings; and mechanisms that rely on the optical and angular momentum properties of non-paraxial beams of light, which do not necessitate couplings beyond dipole transitions.

Whilst the many ways that matter can discriminate the handedness of an optical vortex differ in subtle respects, it emerges that there is a common requirement to engage the sign of OAM. At the individual molecule level we have seen that the key one is the engagement of electric-quadrupole or higher multipolar couplings with the paraxial field. One can go a step further however, and state more generally that interactions dependent on the transverse gradient of the electromagnetic field are requisite; electric quadrupole interactions are the lowest-order of such couplings in paraxial light. The longitudinal fields involved in non-paraxial vortices also stem from the transverse gradients of the electromagnetic field. It is the gradient of the helical-phase that gives optical vortices their OAM, and so it should be of no surprise that in order to engage this property in spectroscopic applications we require the material to interact with this gradient. At the single-photon level these gradients, directly related to optical phase, vary with a steepness that strongly depends on topological charge—as well as a forward propagation phase, and any Gouy phase arising from non-paraxial propagation. At the quantum level, effects that depend on such gradients may be considered a general indication of the delocalised action of the photon (a direct manifestation of wave-particle duality). The necessity for this form of interaction clearly stems from the fact that it engages the helical phase gradient, the only characteristic of a twisted beam of light in which the vortex handedness has a physical manifestation. It is notable that numerous studies have discovered the highly distinct and important role that electric quadrupole interactions with twisted light beams can play, outside of chiral optics [8, 12, 80, 109–111].

Although optical activity with twisted light requires a dependence on the sign of OAM through the vortex handedness, many of the effects outlined in this review also depend on the magnitude of optical OAM. This is another significant and useful feature as it provides for the potential to enhance light–matter interactions, and the usually weak optical activity signals, by adopting an input beam with a large value of ℓ. So-called 'perfect optical vortices' [112–114], which possess a radial intensity profile that is independent of the value of ℓ, are sure to play a particularly important role here as they allow the input value of ℓ to be increased in a spectroscopic application without having to take into account any of the associated intensity profile changes that occur with normal optical vortices.

The principle of coupling to field gradients has an interesting corollary in the case of chiral arrays, as noted in section 2. Cylindrically symmetric arrays of molecules or chromophores, or molecules of such C_n symmetry with side-arms, can support delocalised electronic states that may engage with electric field gradients across their full spatial extent. As has been shown by Zang and Lusk [115, 116], electric quadrupole interactions of the whole, through dipole coupling between the constituent chromophores, can thereby lead to the formation of *twisted excitons*. Quanta of angular momentum with $|\ell| \leqslant n$ are thereby conserved in direct transfer between photonic and excitonic manifestations. Previous work by Coles, Williams *et al* [117, 118] provides similar grounds for the direct emission of optical vortices by the same mechanism. These effects exhibit OAM principles directly analogous (through time-reversal) to the absorption processes described in this review.

It is extremely promising to observe that even in a rather short period of time, the chirality associated with optical vortices has received keen attention as a prospective spectroscopic tool to characterise materials ranging from achiral atomic matter and both chiral and achiral molecules, to plasmonic, nano- and meta-materials. While optical activity and chiroptical spectroscopy is generally studied and utilised in the fields of chemistry, chemical physics, and biochemistry [119, 120], structured light and optical angular momentum topics are deeply embedded in optics and physics. The field of twisted light and optical activity not only offers substantial scope for cross-fertilisation, but necessitates the engagement of both perspectives. With numerous key theoretical paradigms discovered underpinning these effects, alongside the cutting-edge experiments, the field of twisted light and optical activity is sure to be a key player in the field of structured light and optical angular momentum in the coming years.

ORCID iDs

Kayn A Forbes ⬤ https://orcid.org/0000-0002-8884-3496
David L Andrews ⬤ https://orcid.org/0000-0002-5903-0787

References

[1] Rubinsztein-Dunlop H *et al* 2016 Roadmap on structured light *J. Opt.* **19** 013001
[2] Mandel L and Wolf E 1995 *Optical Coherence and Quantum Optics* (Cambridge: Cambridge University Press)
[3] Chipman R A, Lam W S T and Young G 2018 *Polarized Light and Optical Systems* (Boca Raton, FL: CRC Press)
[4] Van Enk S J and Nienhuis G 1994 Spin and orbital angular momentum of photons *EPL* **25** 497
[5] Barnett S M 2010 Rotation of electromagnetic fields and the nature of optical angular momentum *J. Mod. Opt.* **57** 1339–43
[6] Barnett S M, Allen L, Cameron R P, Gilson C R, Padgett M J, Speirits F C and Yao A M 2016 On the natures of the spin and orbital parts of optical angular momentum *J. Opt.* **18** 064004
[7] Simpson N B, Dholakia K, Allen L and Padgett M J 1997 Mechanical equivalence of spin and orbital angular momentum of light: an optical spanner *Opt. Lett.* **22** 52–4
[8] Babiker M, Andrews D L and Lembessis V E 2018 Atoms in complex twisted light *J. Opt.* **21** 013001
[9] Tischler N, Zambrana-Puyalto X and Molina-Terriza G 2012 The role of angular momentum in the construction of electromagnetic multipolar fields *Eur. J. Phys.* **33** 1099
[10] Andrews D L 2010 Optical angular momentum: multipole transitions and photonics *Phys. Rev.* A **81** 033825
[11] Babiker M, Bennett C R, Andrews D L and Romero L D 2002 Orbital angular momentum exchange in the interaction of twisted light with molecules *Phys. Rev. Lett.* **89** 143601
[12] Schmiegelow C T, Schulz J, Kaufmann H, Ruster T, Poschinger U G and Schmidt-Kaler F 2016 Transfer of optical orbital angular momentum to a bound electron *Nat. Commun.* **7** 12998
[13] Afanasev A, Carlson C E, Schmiegelow C T, Schulz J, Schmidt-Kaler F and Solyanik M 2018 Experimental verification of position-dependent angular-momentum selection rules for absorption of twisted light by a bound electron *New J. Phys.* **20** 023032
[14] Schulz S A L, Fritzsche S, Müller R A and Surzhykov A 2019 Modification of multipole transitions by twisted light *Phys. Rev.* A **100** 043416
[15] Bradshaw D S, Leeder J M, Coles M M and Andrews D L 2015 Signatures of material and optical chirality: origins and measures *Chem. Phys. Lett.* **626** 106–10
[16] Arago J D F 1811 Mémoire sur une modification remarquable qu'éprouvent les rayons lumineux dans leur passage à travers certains corps diaphanes, et sur quelques autre nouveaux phénomènes 'd'optique [On an interesting effect shown by light rays on their passage through certain transparent materials, and some other new optical phenomena] *Mém. De l'Inst.* **12** 93–134 (in French)
[17] Biot J B 1817 Mémoire sur les rotations que certaines substances impriment aux axes de polarisation des rayons lumineux *Mem. Acad. Sci.* **2** 41–136 (in French)
[18] Fresnel A 1825 Extrait d'un mémoire sur la double refraction particuliere que presente le cristal de roche dans la direction de son axe *Ann. Chim. Phys.* **28** 147
[19] Hecht E 2015 *Optics* (Harlow: Pearson Education)
[20] Fernandez-Corbaton I, Zambrana-Puyalto X and Molina-Terriza G 2012 Helicity and angular momentum: a symmetry-based framework for the study of light-matter interactions *Phys. Rev.* A **86** 042103
[21] Lazzeretti P 2017 The abstract GPT and GCPT groups of discrete C, P and T symmetries *J. Mol. Spectrosc.* **337** 178–84
[22] Andrews D L 2018 Quantum formulation for nanoscale optical and material chirality: symmetry issues, space and time parity, and observables *J. Opt.* **20** 033003
[23] Craig D P and Thirunamachandran T 1998 *Molecular Quantum Electrodynamics: An Introduction to Radiation-Molecule Interactions* (New York: Courier Corporation)
[24] Salam A 2010 *Molecular Quantum Electrodynamics: Long-range Intermolecular Interactions* (New York: Wiley)
[25] Andrews D L, Jones G A, Salam A and Woolley R G 2018 Perspective: quantum Hamiltonians for optical interactions *J. Chem. Phys.* **148** 040901
[26] Woolley R G 2020 Power-Zienau-Woolley representations of nonrelativistic QED for atoms and molecules *Phys. Rev. Res.* **2** 013206
[27] Forbes K A 2018 Role of magnetic and diamagnetic interactions in molecular optics and scattering *Phys. Rev.* A **97** 053832
[28] Romero L D, Andrews D L and Babiker M 2002 A quantum electrodynamics framework for the nonlinear optics of twisted beams *J. Opt. B: Quantum Semiclass. Opt.* **4** S66–72
[29] Andrews D L 2020 Conceptualization of the photon for quanta of structured light *Proc. SPIE* **11297** 1129702
[30] Lodahl P, Mahmoodian S, Stobbe S, Rauschenbeutel A, Schneeweiss P, Volz J, Pichler H and Zoller P 2017 Chiral quantum optics *Nature* **541** 473
[31] Cheng M T, Ma X, Fan J W, Xu J and Zhu C 2017 Controllable single-photon nonreciprocal propagation between two waveguides chirally coupled to a quantum emitter *Opt. Lett.* **42** 2914–7
[32] Engheta N and Ziolkowski R W 2006 *Metamaterials: Physics and Engineering Explorations* (New York: Wiley)
[33] Zouhdi S, Sihvola A and Vinogradov A P 2008 *Metamaterials and Plasmonics: Fundamentals, Modelling, Applications* (Berlin: Springer)
[34] Mackay T G and Lakhtakia A 2010 Negatively refracting chiral metamaterials: a review *SPIE Rev.* **1** 018003
[35] Costa J T, Silveirinha M G and Alù A 2011 Poynting vector in negative-index metamaterials *Phys. Rev.* B **83** 165120
[36] Coles M M and Andrews D L 2012 Chirality and angular momentum in optical radiation *Phys. Rev.* A **85** 063810

[37] Omatsu T, Miyamoto K, Toyoda K, Morita R, Arita Y and Dholakia K 2019 A new twist for materials science: the formation of chiral structures using the angular momentum of light *Adv. Opt. Mater.* **7** 1801672

[38] Bliokh K Y and Nori F 2015 Transverse and longitudinal angular momenta of light *Phys. Rep.* **592** 1–38

[39] Afanasiev G N 1994 Vector solutions of the Laplace equation and the influence of helicity on Aharonov-Bohm scattering *J. Phys. A: Math. Gen.* **27** 2143

[40] Crimin F, Mackinnon N, Götte J B and Barnett S M 2019 Optical helicity and chirality: conservation and sources *Appl. Sci.* **9** 828

[41] Parchaňskỳ V, Kapitan J and Bouř P 2014 Inspecting chiral molecules by Raman optical activity spectroscopy *RSC Adv.* **4** 57125–36

[42] Forbes K A and Andrews D L 2019 Enhanced optical activity using the orbital angular momentum of structured light *Phys. Rev. Res.* **1** 033080

[43] Stephens P J and Lowe M A 1985 Vibrational circular dichroism *Annu. Rev. Phys. Chem.* **36** 213–41

[44] Barron L D 2009 *Molecular Light Scattering and Optical Activity* (Cambridge: Cambridge University Press)

[45] Barron L D and Buckingham A D 2010 Vibrational optical activity *Chem. Phys. Lett.* **492** 199–213

[46] Andrews D L, Romero L D and Babiker M 2004 On optical vortex interactions with chiral matter *Opt. Commun.* **237** 133–9

[47] Araoka F, Verbiest T, Clays K and Persoons A 2005 Interactions of twisted light with chiral molecules: an experimental investigation *Phys. Rev.* A **71** 055401

[48] Allen L 2017 Orbital angular momentum: a personal memoir *Phil. Trans. R. Soc.* A **375** 20160280

[49] Forbes K A and Andrews D L 2018 Optical orbital angular momentum: twisted light and chirality *Opt. Lett.* **43** 435–8

[50] Bekshaev A, Bliokh K Y and Soskin M 2011 Internal flows and energy circulation in light beams *J. Opt.* **13** 053001

[51] Forbes K A and Andrews D L 2019 Spin-orbit interactions and chiroptical effects engaging orbital angular momentum of twisted light in chiral and achiral media *Phys. Rev.* A **99** 023837

[52] Forbes K A and Salam A 2019 Kramers-Heisenberg dispersion formula for scattering of twisted light *Phys. Rev.* A **100** 053413

[53] Power E A and Thirunamachandran T 1974 Circular dichroism: a general theory based on quantum electrodynamics *J. Chem. Phys.* **60** 3695–701

[54] Ye L, Rouxel J R, Asban S, Rösner B and Mukamel S 2019 Probing molecular chirality by orbital angular momentum carrying X-ray pulses *J. Chem. Theory Comput.* **15** 4180–6

[55] Forbes K A 2019 Raman optical activity using twisted photons *Phys. Rev. Lett.* **122** 103201

[56] Bisson J F, Miyamoto K and Omatsu T 2019 Power-scalable and high-speed orbital angular momentum modulator *Japan. J. Appl. Phys.* **58** 032009

[57] Li H and Nafie L A 2012 Simultaneous acquisition of all four forms of circular polarization Raman optical activity: results for α-pinene and lysozyme *J. Raman Spectrosc.* **43** 89–94

[58] McArthur D, Yao A M and Papoff F 2020 Scattering of light with angular momentum from an array of particles *Phys. Rev. Res.* **2** 013100

[59] Mamani S, Shi L, Ahmed T, Karnik R, Rodríguez-Contreras A, Nolan D and Alfano R 2018 Transmission of classically entangled beams through mouse brain tissue *J. Biophotonics* **11** e201800096

[60] Milione G, Secor J, Michel G, Evans S and Alfano R R 2011 Raman optical activity by light with spin and orbital angular momentum *Proc. SPIE* **7950** 79500H

[61] Bendau E, Zhang L, Gozali R, Ashrafi S and Alfano R R 2017 Vortex beams and optical activity of sucrose *Proc. SPIE* **10120** 1012004

[62] Forbes K A 2020 Nonlinear chiral molecular photonics using twisted light: hyper-Rayleigh and hyper-Raman optical activity *J. Opt.* **22** 095401

[63] Leach J, Keen S, Padgett M J, Saunter C and Love G D 2006 Direct measurement of the skew angle of the Poynting vector in a helically phased beam *Opt. Express* **14** 11919–24

[64] Rumala Y S and Leanhardt A E 2017 Optical vortex with a small core and Gaussian intensity envelope for light-matter interaction *J. Opt. Soc. Am.* B **34** 909–18

[65] Arikawa T, Morimoto S and Tanaka K 2017 Focusing light with orbital angular momentum by circular array antenna *Opt. Express* **25** 13728–35

[66] Canós Valero A, Kislov D, Gurvitz E A, Shamkhi H K, Pavlov A A, Redka D, Yankin S, Zemánek P and Shalin A S 2019 Nanovortex-driven all-dielectric optical diffusion boosting and sorting concept for lab-on-a-chip platforms *Adv. Sci.* **7** 1903049

[67] Shutova M, Shutov A D and Sokolov A V 2020 Spectroscopic sensing enhanced by quantum molecular coherence and by plasmonic nanoantennas *Proc. SPIE* **11296** 1129605

[68] Ni J *et al* 2021 Gigantic vortical differential scattering as a monochromatic probe for multiscale chiral structures *Proc. Natl. Acad. Sci. USA* **118** e2020055118

[69] Paroli B, Siano M and Potenza M A C 2019 The local intrinsic curvature of wavefronts allows to detect optical vortices *Opt. Express* **27** 17550–60

[70] Mason W R 2006 *A Practical Guide to Magnetic Circular Dichroism Spectroscopy* (Hoboken, NJ: John Wiley & Sons, Inc)

[71] van Veenendaal M and McNulty I 2007 Prediction of strong dichroism induced by x rays carrying orbital momentum *Phys. Rev. Lett.* **98** 157401

[72] Mathevet R, de Lesegno B V, Pruvost L and Rikken G L 2013 Negative experimental evidence for magneto-orbital dichroism *Opt. Express* **21** 3941–5

[73] Sirenko A A, Marsik P, Bernhard C, Stanislavchuk T N, Kiryukhin V and Cheong S W 2019 Terahertz vortex beam as a spectroscopic probe of magnetic excitations *Phys. Rev. Lett.* **122** 237401

[74] Fanciulli M, Bresteau D, Vimal M, Luttmann M, Sacchi M and Ruchon T 2020 Electromagnetic theory of helicoidal dichroism in reflection from magnetic structures *Phys. Rev.* A **103** 013501

[75] Collins J T, Kuppe C, Hooper D C, Sibilia C, Centini M and Valev V K 2017 Chirality and chiroptical effects in metal nanostructures: fundamentals and current trends *Adv. Opt. Mater.* **5** 1700182

[76] Hentschel M, Schäferling M, Duan X, Giessen H and Liu N 2017 Chiral plasmonics *Sci. Adv.* **3** e1602735

[77] Lee Y Y, Kim R M, Im S W, Balamurugan M and Nam K T 2020 Plasmonic metamaterials for chiral sensing applications *Nanoscale* **12** 58–66

[78] Wu T, Wang R and Zhang X 2015 Plasmon-induced strong interaction between chiral molecules and orbital angular momentum of light *Sci. Rep.* **5** 18003

[79] Guo Y, Zhu G, Bian W, Dong B and Fang Y 2020 Orbital angular momentum dichroism caused by the interaction of electric and magnetic dipole moments and the geometrical asymmetry of chiral metal nanoparticles *Phys. Rev.* A **102** 033525

[80] Brullot W, Vanbel M K, Swusten T and Verbiest T 2016 Resolving enantiomers using the optical angular momentum of twisted light *Sci. Adv.* **2** e1501349
[81] Ren H and Gu M 2018 Angular momentum-reversible near-unity bisignate circular dichroism *Laser Photonics Rev.* **12** 1700255
[82] Wang S, Deng Z L, Cao Y, Hu D, Xu Y, Cai B, Jin L, Bao Y, Wang X and Li X 2018 Angular momentum-dependent transmission of circularly polarized vortex beams through a plasmonic coaxial nanoring *IEEE Photon. J.* **10** 1–9
[83] Reddy I V, Baev A, Furlani E P, Prasad P N and Haus J W 2018 Interaction of structured light with a chiral plasmonic metasurface: giant enhancement of chiro-optic response *ACS Photonics* **5** 734–40
[84] Arikawa T, Hiraoka T, Morimoto S, Blanchard F, Tani S, Tanaka T, Sakai K, Kitajima H, Sasaki K and Tanaka K 2020 Transfer of orbital angular momentum of light to plasmonic excitations in metamaterials *Sci. Adv.* **6** eaay1977
[85] Zhang X and Cui T J 2020 Single-particle dichroism using orbital angular momentum in a microwave plasmonic resonator *ACS Photonics* **7** 3291–7
[86] Bekshaev A, Soskin M and Vasnetsov M 2008 *Paraxial Light Beams with Angular Momentum* (New York: Nova Science Publishers)
[87] Zangwill A 2013 *Modern Electrodynamics* (Cambridge: Cambridge University Press)
[88] Andrews D L and Babiker M (eds) 2012 *The Angular Momentum of Light* (Cambridge: Cambridge University Press) (https://doi.org/10.1017/CBO9780511795213)
[89] Lax M, Louisell W H and McKnight W B 1975 From Maxwell to paraxial wave optics *Phys. Rev. A* **11** 1365
[90] Davis L W 1979 Theory of electromagnetic beams *Phys. Rev. A* **19** 1177
[91] Novotny L and Hecht B 2012 *Principles of Nano-Optics* (Cambridge: Cambridge University Press)
[92] Klimov V, Bloch D, Ducloy M and Leite J R R 2009 Detecting photons in the dark region of Laguerre-Gauss beams *Opt. Express* **17** 9718–23
[93] Quinteiro G F, Schmidt-Kaler F and Schmiegelow C T 2017 Twisted-light–ion interaction: the role of longitudinal fields *Phys. Rev. Lett.* **119** 253203
[94] Nechayev S, Eismann J S, Leuchs G and Banzer P 2019 Orbital-to-spin angular momentum conversion employing local helicity *Phys. Rev. B* **99** 075155
[95] Bliokh K Y, Alonso M A, Ostrovskaya E A and Aiello A 2010 Angular momenta and spin-orbit interaction of nonparaxial light in free space *Phys. Rev. A* **82** 063825
[96] Bliokh K Y, Rodríguez-Fortuño F J, Nori F and Zayats A V 2015 Spin–orbit interactions of light *Nat. Photon.* **9** 796–808
[97] Löffler W, Broer D J and Woerdman J P 2011 Circular dichroism of cholesteric polymers and the orbital angular momentum of light *Phys. Rev. A* **83** 065801
[98] Löffler W, Van Exter M P, Nienhuis G, Broer D J and Woerdman J P 2011 Search for Hermite-Gauss mode rotation in cholesteric liquid crystals *Opt. Express* **19** 12978–83
[99] Zambrana-Puyalto X, Vidal X and Molina-Terriza G 2014 Angular momentum-induced circular dichroism in non-chiral nanostructures *Nat. Commun.* **5** 4922
[100] Bokor N, Iketaki Y, Watanabe T and Fujii M 2005 Investigation of polarization effects for high-numerical-aperture first-order Laguerre-Gaussian beams by 2D scanning with a single fluorescent microbead *Opt. Express* **13** 10440
[101] Kindler J, Banzer P, Quabis S, Peschel U and Leuchs G 2007 Waveguide properties of single subwavelength holes demonstrated with radially and azimuthally polarized light *Appl. Phys. B* **89** 517–20
[102] De Abajo F G 2007 Colloquium: light scattering by particle and hole arrays *Rev. Mod. Phys.* **79** 1267
[103] Zambrana-Puyalto X, Vidal X, Woźniak P, Banzer P and Molina-Terriza G 2018 Tailoring multipolar Mie scattering with helicity and angular momentum *ACS Photonics* **5** 2936–44
[104] Samlan C T, Suna R R, Naik D N and Viswanathan N K 2018 Spin-orbit beams for optical chirality measurement *Appl. Phys. Lett.* **112** 031101
[105] Kerber R M, Fitzgerald J M, Oh S S, Reiter D E and Hess O 2018 Orbital angular momentum dichroism in nanoantennas *Commun. Phys.* **1** 87
[106] Afanasev A, Carlson C E and Solyanik M 2017 Circular dichroism of twisted photons in non-chiral atomic matter *J. Opt.* **19** 105401
[107] Woźniak P, Leon I D, Höflich K, Leuchs G and Banzer P 2019 Interaction of light carrying orbital angular momentum with a chiral dipolar scatterer *Optica* **6** 961–5
[108] Rosales-Guzmán C, Volke-Sepulveda K and Torres J P 2012 Light with enhanced optical chirality *Opt. Lett.* **37** 3486–8
[109] Lembessis V E and Babiker M 2013 Enhanced quadrupole effects for atoms in optical vortices *Phys. Rev. Lett.* **110** 083002
[110] Ji Z, Liu W, Krylyuk S, Fan X, Zhang Z, Pan A, Feng L, Davydov A and Agarwal R 2020 Photocurrent detection of the orbital angular momentum of light *Science* **368** 763–7
[111] Bougouffa S and Babiker M 2020 Atom trapping and dynamics in the interaction of optical vortices with quadrupole-active transitions *Phys. Rev. A* **101** 043403
[112] Ostrovsky A S, Rickenstorff-Parrao C and Arrizón V 2013 Generation of the "perfect" optical vortex using a liquid-crystal spatial light modulator *Opt. Lett.* **38** 534–6
[113] Chen Y, Fang Z X, Ren Y X, Gong L and Lu R D 2015 Generation and characterization of a perfect vortex beam with a large topological charge through a digital micromirror device *Appl. Opt.* **54** 8030–5
[114] Yu J, Miao C, Wu J and Zhou C 2020 Circular Dammann gratings for enhanced control of the ring profile of perfect optical vortices *Photon. Res.* **8** 648–58
[115] Zang X and Lusk M T 2017 Angular momentum transport with twisted exciton wave packets *Phys. Rev. B* **96** 155104
[116] Zang X and Lusk M T 2017 Twisted molecular excitons as mediators for changing the angular momentum of light *Phys. Rev. A* **96** 013819
[117] Coles M M, Williams M D, Saadi K, Bradshaw D S and Andrews D L 2013 Chiral nanoemitter array: a launchpad for optical vortices *Laser Photonics Rev.* **7** 1088–92
[118] Williams M D, Coles M M, Bradshaw D S and Andrews D L 2014 Direct generation of optical vortices *Phys. Rev. A* **89** 033837
[119] Berova N, Polavarapu P L, Nakanishi K and Woody R W 2011 *Comprehensive Chiroptical Spectroscopy: Instrumentation, Methodologies, and Theoretical Simulations* vol 1 (New York: Wiley)
[120] Berova N, Polavarapu P L, Nakanishi K and Woody R W 2012 *Comprehensive Chiroptical Spectroscopy: Applications in Stereochemical Analysis of Synthetic Compounds, Natural Products, and Biomolecules* vol 2 (New York: Wiley)